



UvA-DARE (Digital Academic Repository)

Organic carbon cycling in a Caribbean coral reef

Hidden biomass, sneezing sponges, and net heterotrophy

Kornder, N.A.

Publication date

2023

[Link to publication](#)

Citation for published version (APA):

Kornder, N. A. (2023). *Organic carbon cycling in a Caribbean coral reef: Hidden biomass, sneezing sponges, and net heterotrophy*. [Thesis, fully internal, Universiteit van Amsterdam].

General rights

It is not permitted to download or to forward/distribute the text or part of it without the consent of the author(s) and/or copyright holder(s), other than for strictly personal, individual use, unless the work is under an open content license (like Creative Commons).

Disclaimer/Complaints regulations

If you believe that digital publication of certain material infringes any of your rights or (privacy) interests, please let the Library know, stating your reasons. In case of a legitimate complaint, the Library will make the material inaccessible and/or remove it from the website. Please Ask the Library: <https://uba.uva.nl/en/contact>, or a letter to: Library of the University of Amsterdam, Secretariat, P.O. Box 19185, 1000 GD Amsterdam, The Netherlands. You will be contacted as soon as possible.



Chapter

4

Carbon cycling in a coral reef: I. External subsidies sustain net heterotrophy despite high primary productivity

Niklas A Kornder, Anna J Rombouts, William J Barnes, Amber T K Riley, Mark J A Vermeij, Jef Huisman, Jasper M de Goeij

In preparation for submission

ABSTRACT

Coral reefs are historically known to achieve high productivity in oligotrophic waters. This is often attributed to effective assimilation of organic carbon (C) by the primary producers on the reef and efficient retention of C by a diverse community of heterotrophic organisms. Yet, our quantitative understanding of the major C fluxes within present-day coral reef communities is still limited. For example, the contributions of organisms inhabiting cryptic habitats (e.g., caves, crevices, overhangs) are often not included, even though their biomass can match that of organisms in exposed reef locations. Furthermore, recently discovered fluxes, such as the turnover of dissolved organic matter into detritus by sponges, are rarely considered in models of carbon cycling on coral reefs. To better understand the organic C fluxes in present-day reef communities, we included such recent insights in a linear-inverse model representing known and presumed C fluxes of the shallow-water (10 m water depth) reef communities surrounding a small Caribbean island (Curaçao). The model is based on productivity and respiration rates, and net fluxes of planktonic, detrital, and dissolved organic carbon measured in 192 *in-situ* incubations of common benthic reef organisms, combined with published data. Our model confirmed the high gross primary productivity (GPP) of Caribbean coral reefs ($1.9 \pm 0.4 \text{ mol C m}^{-2} \text{ d}^{-1}$), but found that respiratory demands (R) were even higher than GPP in the studied reefs (daily P:R ratio = 0.84 ± 0.05). Also, the total biomass of the heterotrophic organisms in the reef communities was slightly higher than the total biomass of the autotrophic organisms. Excess respiration was made possible by allochthonous carbon subsidies, mainly in the form of dissolved organic matter (DOM) and plankton taken up from the water column above the reef. The total standing biomass of Curaçaoan reef communities was 8 % of their annual GPP, which aligns with estimates from several other reef ecosystems around the globe spanning a period of several decades. A large fraction of the organic carbon produced by autotrophs ($22 \pm 8 \%$) was released as DOM, but retained within reef communities by sponges and the microbial loop. Our analysis sheds new light on the organic carbon fluxes in a present-day coral reef and may provide a possible benchmark to assess how carbon sequestration, and accompanying ecological functions, might change in future coral reef communities.

INTRODUCTION

Coral reefs are complex ecosystems harboring a wide array of taxa with different nutritional strategies and occupying different functional niches (Paulay 1997; Reaka-Kudla 1997; Harmelin-Vivien 2002). Their gross primary productivity (GPP) has been estimated to generally range between 200 and 500 mmol organic carbon (C) m⁻² d⁻¹ (Hatcher 1988), although some reefs were shown to produce up to 2750 mmol C m⁻² d⁻¹ (Adey and Steneck 1985). This productivity approaches or even exceeds the GPP of agricultural crops, despite the low concentrations of nutrients in coral reef waters (Hatcher 1988; Gilmanov et al. 2010). Early studies indicated that the primary production on coral reefs was foremost recycled and used within the community that produced them (Odum and Odum 1955; Kinsey 1983), so that reefs' GPP was approximately similar to their respiration (R) and excess production was close to zero (Margalef 1974; Hatcher 1990; Crossland et al. 1991). This balance was attributed to efficient use of limited resources (e.g., nitrogen, phosphorus) and efficient recycling of primary production by a varied and large heterotrophic community (e.g., fish, sponges, sea urchins) (Odum and Odum 1955; Kinsey 1983; de Goeij et al. 2013). The efficient use of resources enables the development of a highly productive coral reef community, providing ecosystem services and economic value to humans through coastal protection, food production and tourism (Reaka-Kudla 1997; Moberg and Folke 1999; Cesar et al. 2003; Burke and Maidens 2004).

The composition of coral reef communities has changed considerably over the last few decades due to anthropogenic stressors (Nyström et al. 2000; Wilson et al. 2006; Bruno et al. 2009; Hughes et al. 2017b; Eakin et al. 2019; Cornwall et al. 2021). Historically, scleractinian corals, coralline algae, and herbivorous fishes were important functional groups shaping the composition of coral reef communities (Ogden 1976; Mumby and Steneck 2008). Over the past decades a general reduction in the abundance of reef-building calcifying taxa (e.g., scleractinian corals and coralline algae) occurred in many locations, whereas the abundance of non-reef-building taxa (e.g., fleshy macroalgae, gorgonians) increased (Gardner et al. 2003; Jackson et al. 2014; Reverter et al. 2022). The abundance of macroalgae has, for example, increased due to overfishing of herbivorous fish and eutrophication (Jackson et al. 2014). The altered abundances of producers and consumers likely affect a variety of ecological processes shaping reef communities, their net productivity, and the degree to which primary products are locally recycled (Kennedy et al. 2013; McWilliam et al. 2020; Nagelkerken et al. 2020; Tebbett and Bellwood 2021).

While changes in community composition of coral reefs have been well documented, we know surprisingly little of how these changes have affected carbon sequestration and the amounts and types of organic carbon (e.g., dissolved

versus particulate, living versus detrital) that are exchanged among various reef organisms (Davis et al. 2021). Several major fluxes of carbon were not even known until recently, such as the large uptake rate of dissolved organic matter by sponges (e.g., de Goeij et al. 2013) or the extent of microbial cycling of carbon (e.g., Nelson et al. 2013; Haas et al. 2016). Moreover, changes in carbon flows within the community may affect the abundances of organisms relying on certain sources of organic carbon for food. For example, macroalgae release more DOM than Caribbean corals, but also with a higher bioavailability (so-called “labile” DOM) to microbes (Nelson et al. 2013) and sponges (Rix et al. 2017; Campana et al. 2021). The increased abundance of macroalgae could thus result in an increased abundance of organisms that consume DOM, such as sponges and microbes, leading to increased availability of sponge-produced detritus through the sponge loop (de Goeij et al. 2013) and negative feedback loops mediated through microbes, such as the DDAM pathway (DOM–death or disease–algae–microbes) (Rohwer et al. 2010; Haas et al. 2016). Hence, understanding altered carbon fluxes not only provides insight into processes shaping reef community composition, but also provides critical information on how communities may further develop on coral reefs in the future.

4 In addition, many reef organisms remain generally underrepresented in most benthic community assessments, such as the so-called cryptic communities living under or even within coral reef structures. The still limited knowledge of these communities further complicates our understanding of carbon budgets and flows within present-day Caribbean reef communities. The biomass of cryptic communities is often severely underestimated, as cryptic habitats are largely invisible in classic reef surveys based on 2D photo-surveys of the exposed reef community (Kornder et al. 2021). The composition of the cryptic community (Kornder et al. 2021) and its ecological function (e.g., Richter et al. 2001; de Goeij and van Duyl 2007) are markedly different from the community on the exposed parts of the reef. The cryptic reef community can account for half of the standing biomass of present-day Caribbean reef communities (Kornder et al. 2021). Since the cryptobenthos consumes large amounts of plankton (Gast et al. 1998; Richter et al. 2001; Scheffers et al. 2004) and dissolved organic matter (DOM) (de Goeij and van Duyl 2007; de Goeij et al. 2013), it needs to be included in the carbon budgets of the entire benthic reef community to quantify e.g., the proportion of producers versus consumers (Trebilco et al. 2013; Simpfendorfer and Heupel 2016; Bradley et al. 2017) or the turnover time of carbon within the total reef community (Margalef 1963; Odum 1985; Christensen 1995; Ainsworth and Mumby 2015; Schramski et al. 2015; Argüelles-Jiménez et al. 2021).

The high biodiversity of reef communities makes for a large number of potential trophic links between producers and consumers. This makes it difficult to estimate

the extent to which different species contribute to the total community's metabolism and carbon flows (Hatcher 1997; Bierwagen et al. 2018). Determination of all possible producer-consumer flows among all coral reef species would pose enormous practical problems. Nevertheless, estimates of carbon production and consumption rates (e.g., respiration, productivity, grazing) for representative species of different functional groups and standing stocks of carbon sources (e.g., DOM, detritus, plankton) can be measured, or are available in the literature. In such cases, where only limited data are available, linear inverse models (LIMs) can be used to constrain and explore the major fluxes in food webs and other ecological networks (Hannon 1973; Polovina 1984; Allesina and Bondavalli 2003; Soetaert and van Oevelen 2009; van Oevelen et al. 2009). For this purpose, a network of the relevant functional groups and organic matter pools is defined by a system of differential equations. The major fluxes between different members in this network are balanced by solving the differential equations for equilibrium, thereby assuming that the entire network is in "steady state". Although benthic communities may display complex non-equilibrium dynamics (Benincà et al. 2015), the assumption of steady states can be a useful first approach in food web models of coral reefs, where the uncertainties associated with measured fluxes are generally high (Odum and Odum 1955; Hiatt and Strasburg 1960; Opitz 1996; van Oevelen et al. 2006; Cáceres et al. 2016).

In this study, we used a LIM approach to summarize existing information, in order to improve our understanding of the most important pathways and taxa involved in carbon production and consumption in shallow-water Caribbean coral reef communities. For this purpose, we constructed a model to describe the carbon flows within and between different functional groups inhabiting the leeward fringing reefs on the Caribbean island of Curaçao. In total, the model consisted of 14 differential equations comprising 78 carbon flows (Box 1). To calibrate the model, we measured the ranges of net fluxes of dissolved oxygen and dissolved and particulate C in 192 *in-situ* incubations of a wide variety of reef organisms (e.g., scleractinian corals, gorgonians, coralline algae, non-calcifying algae, sponges; summarized in Table 1). Additional carbon fluxes and hydrodynamic parameters were obtained from the literature (Table S1). We then combined these data with local abundance estimates of the benthic and pelagic functional groups to estimate the reef community's mean gross and net metabolic fluxes, as well as the C flows between all major members of benthic and pelagic reef communities.

METHODS

Model construction & analysis

We use a linear inverse model (LIM; Kones et al. 2009; Soetaert and van Oevelen 2009) to describe flows of organic carbon (C) between different benthic communities of the reef ecosystem within a 1 x 1 m reef section (including the overlying 10 m water column and the underlying cryptic habitat) using a set of mass balance equations (Box 1). In total, the model consists of 14 differential equations, representing the 11 major functional groups in the studied coral reef community (scleractinian corals, coralline algae, non-calcifying algae (including macroalgae, turf algae and benthic cyanobacterial mats), cryptic mixed communities, coral rock communities, sediment communities, fishes, gorgonians, motile invertebrates, encrusting sponges, and massive sponges) and 3 pelagic pools of organic matter (DOM, detritus, plankton). Fluxes of carbon mediated by these functional groups are described by 78 carbon flows that capture nine qualitatively different biological processes: GPP, respiration, DOM production, DOM consumption, detritus production, detritus consumption, grazing on plankton, grazing on non-calcifying algae (herbivory), and (non-herbivorous) predation. Furthermore, our LIM considers the inflow and outflow of suspended organic C by the ocean current above the reef, replenishing the pool of organic C in the 10-m water column of our model space. Part of the organic C inflow is consumed by the reef organisms (described as “import” into the reef community) and part of the outflow is produced by the reef organisms (described as “export” from the reef community).

Under the assumption of steady state, the LIM solves the mass balance equations to calculate the C flows in the system. To constrain our calculation of the C flows, the C flows mediated by the 11 different functional groups (in $\text{mmol C m}^{-2} \text{d}^{-1}$) were also estimated from the product of the biomass of each of the functional groups and its species-specific C fluxes (data on C fluxes were derived from several species per group; see Tables 1 and S1). Biomasses of the functional groups were measured at the reef slopes at 12 sites along the leeward coast of the Caribbean island of Curaçao (WAITT-Institute 2017; Kornder et al. 2021). Motile invertebrates were not included in this dataset, and therefore their abundance was assumed to equal estimates from nearby Honduran coral reefs (404 gww m^{-2}) (Cáceres et al. 2016). Species-specific C fluxes were measured in field incubations (see below), except for C fluxes of sponges, motile invertebrates, and fish, which were obtained from the published literature (Table S1). Published estimates of respiration by massive sponges were supplemented with *in-situ* measurements (Table S2, $n = 20$, see Supplementary methods). Variability in these measurements and literature data was taken into account by computing 95-percentile limits for

each of the C flows in the model. When less than 5 estimates were available, the minimum and maximum values were used instead of the 95-percentiles. These 95-percentile limits and min-max values were entered into the LIM to constrain the range of possible values for each C flow. Model solutions were generated for each C flow by running the LIM 9999 times with random initial sampling from the defined ranges using Markov-Chain-Monte-Carlo simulations. For each model solution, community fluxes of GPP, R, and other whole-community C fluxes were calculated by summing the C flows of the individual functional groups. All C flows estimated from these simulations were summarized as their mean \pm SD and their 95-percentile range. Our model was built in R (R Core Team 2021) using the package *LIM*, and solved with the function “*xsample*” (Soetaert and van Oevelen 2009).

We analyzed our model outputs to quantify the fluxes of carbon to, from, and between the functional groups, but also to quantify contributions of autotrophic versus heterotrophic organisms to the total standing biomass (mean \pm SE: 56 ± 13 mol C m⁻² for the studied Caribbean reefs in Curaçao) (Kornder et al. 2021). For this purpose, the biomasses of known sessile mixotrophs (e.g., corals, sponges) were partitioned according to the relative proportions of autotrophy versus heterotrophy in their total C uptake as determined by the model. The contributions of the different sessile functional groups were then summed to estimate the total autotrophic versus heterotrophic biomass in the benthic community. Heterotrophic motile animals (e.g., fish, crustaceans) were summed separately. Finally, we calculated the turnover time of C by dividing the total standing biomass by the annual GPP of the community (in mmol C m⁻² yr⁻¹). For simplicity, the annual GPP was calculated as 365 times the daily GPP as determined by our model, thus neglecting seasonal variability in reef community biomass and carbon fluxes, although our LIM input data was gathered during different seasons and years to capture some temporal variability (see Supplementary methods). We compared the community turnover time of C to various other tropical reefs, for which both the standing biomasses and annual GPP of the community have been reported (Polovina 1984; Opitz 1996; Arias-González et al. 2004; Cáceres et al. 2016).

Box 1. The model consists of a series of ordinary differential equations for coralline algae (ca), cryptic mixed communities (cm), coral rock communities (cr), encrusting sponges (es), fishes (f), gorgonians (gc), motile invertebrates (mi), massive sponges (ms), non-calcifying algae (nca), sediment communities (s), scleractinian corals (sc), plankton (pl), detritus (det), and dissolved organic matter (dom). Carbon flows specified in the model (in $\text{mmol C m}^{-2} \text{d}^{-1}$) are total rates derived by multiplying specific carbon uptake (or release) rates with species abundances on the reef. GPP, gross primary productivity; R, respiration; DOMC, DOM consumption; DOMP, DOM production; DC, detritus consumption; DP, detritus production; PLG, grazing on plankton; AG, grazing on non-calcifying algae; PR, predation. Inflows and outflows of C at the model boundary are derived from seawater C concentrations, hydrodynamic parameters, and C processing by sponges and plankton. IN, total inflow; OUT, total outflow. Double indices (x,y) denote transfer from x to y. The model assumes mass balance, i.e., the differential equations are solved for steady state. For instance, carbon acquired by coralline algae (ca, see first equation in Box 1) via photosynthesis (GPP_{ca}) and uptake of dissolved organic matter ($DOMC_{ca}$) is assumed to equal carbon losses from respiration (R_{ca}) and release of dissolved ($DOMP_{ca}$) and particulate (DP_{ca}) organic matter.

Reef community:

$$\frac{dca}{dt} = 0 = GPP_{ca} - R_{ca} + DOMC_{ca} - DOMP_{ca} - DP_{ca}$$

$$\frac{dcm}{dt} = 0 = GPP_{cm} - R_{cm} + PLG_{cm} + DOMC_{cm} - DOMP_{cm} - DP_{cm}$$

$$\frac{dcr}{dt} = 0 = GPP_{cr} - R_{cr} + PLG_{cr} + DOMC_{cr} - DOMP_{cr} - DP_{cr}$$

$$\frac{des}{dt} = 0 = GPP_{es} - R_{es} + PLG_{es} + DOMC_{es} - DP_{es}$$

$$\frac{df}{dt} = 0 = -R_f + PR_{mi,f} + PR_{ms,f} + PR_{sc,f} + AG_f + PLG_f + DC_f - PR_{f,mi} - DP_f$$

$$\frac{dgc}{dt} = 0 = GPP_{gc} - R_{gc} + PLG_{gc} - DOMP_{gc} - DP_{gc}$$

$$\frac{dmi}{dt} = 0 = -R_{mi} + PR_{f,mi} + PR_{ms,mi} + PR_{sc,mi} + AG_{mi} + PLG_{mi} + DC_{mi} - PR_{mi,f} - DP_{mi}$$

$$\frac{dms}{dt} = 0 = GPP_{ms} - R_{ms} - PR_{ms,f} - PR_{ms,mi} + PLG_{ms} + DOMC_{ms} + DC_{ms} - DOMP_{ms} - DP_{ms}$$

$$\frac{dnca}{dt} = 0 = GPP_{nca} - R_{nca} + DOMC_{nca} - AG_{mi} - AG_f - DOMP_{nca}$$

$$\frac{ds}{dt} = 0 = GPP_s - R_s + DOMC_s + DC_s - DOMP_s$$

$$\frac{dsc}{dt} = 0 = GPP_{sc} - R_{sc} - PR_{sc,f} - PR_{sc,mi} + PLG_{sc} + DOMC_{sc} + DC_{sc} - DOMP_{sc} - DP_{sc}$$

Pelagic carbon pools:

$$\frac{dpl}{dt} = 0 = IN_{pl} + GPP_{pl} - R_{pl} - PLG_{es} - PLG_f - PLG_{mi} - PLG_{ms} - PLG_{sc} - PLG_{gc} - PLG_{cr} - PLG_{cm} + DOMC_{pl} - DOMP_{pl} - DP_{pl} - OUT_{pl}$$

$$\frac{ddet}{dt} = 0 = IN_{det} - DC_{mi} - DC_{ms} - DC_{sc} - DC_s - DC_f - DOMP_{det} + DP_{mi} + DP_{es} + DP_{ms} + DP_{pl} + DP_{sc} + DP_{gc} + DP_{ca} + DP_{cr} + DP_{cm} + DP_f - OUT_{det}$$

$$\frac{ddom}{dt} = 0 = IN_{dom} - DOMC_{ca} - DOMC_{cm} - DOMC_{cr} - DOMC_{es} - DOMC_{ms} - DOMC_{nca} - DOMC_{pl} - DOMC_s - DOMC_{sc} + DOMP_{ms} + DOMP_{sc} + DOMP_{gc} + DOMP_{ca} + DOMP_{nca} + DOMP_{cr} + DOMP_{cm} + DOMP_s + DOMP_{pl} + DOMP_{det} - OUT_{dom}$$

Estimation of C fluxes using field incubations

Field incubations of species representing the different functional groups were used to obtain ranges of the C fluxes of these groups to calibrate the LIM. Detailed methodology for obtaining species-specific carbon flows is provided in the Supplementary methods. Briefly, for our analyses of GPP and respiration, changes in dissolved oxygen (O₂) concentrations were measured once per minute during 3–4 h incubations using optical oxygen probes (Onset HOBO Pendant U-26, calibrated using a two-point calibration of 0 and 100 % O₂ seawater solutions). Concentrations of suspended particulate organic C were analyzed on a CHNS elemental analyzer (Vario El Cube, Elementar, Germany). Dissolved organic C concentrations were measured using a total organic carbon analyzer (TOC-Vcph-TNM-1 autoanalyzer, Shimadzu, Japan) as described by Campana et al. (2021). Plankton abundances were quantified by counting pelagic bacteria and phytoplankton on a flow cytometer (CytoFLEX, Beckman Coulter, USA). Cell numbers were converted to C using published conversion factors (*Synechococcus*: 250 fg C cell⁻¹, *Prochlorococcus*: 53 fg C cell⁻¹ (Campbell et al. 1994), bacteria: 20 fg C cell⁻¹ (Ducklow et al. 1993). All species-specific carbon fluxes (see Table 1) were converted to mmol C per projected m² per h, using published estimates of the species abundances (Kornder et al. 2021). To achieve this, the abundances of organisms in the incubation chambers were expressed in the same units that were measured on the reef in Kornder et al. (2021), i.e., g of ash-free dry weight (AFDW) for macroalgae, cm³ of tissue volume for gorgonians, and cm² of 3D surface area for all other sessile functional groups. As an example, specific C fluxes by corals were expressed as mmol C cm⁻² h⁻¹ and multiplied with coral abundance on the reef in cm² m⁻² to obtain total rates of C flows by corals in mmol C m⁻² h⁻¹.

Consumption and production of plankton, detritus, and dissolved organic C

Daily rates of consumption and production of organic C (DOMC, DOMP, DC, DP and PLG in Box 1) were estimated for each functional group from hourly rates. For this purpose, the total hourly rates (in mmol C m⁻² d⁻¹) determined in the light and in the dark were both multiplied by 12 h, assuming a 12:12 h day-night cycle.

Hourly fluxes of planktonic, detrital, and dissolved organic C consumed and/or produced by the plankton community were determined from incubations containing unfiltered seawater at 10 m water depth (light: n = 18, dark: n = 14). Thereto, the concentrations of planktonic, detrital, and dissolved organic C inside the incubation chambers were linearly regressed against time. The regression slopes (s, in mmol C h⁻¹) obtained from the incubation chambers (3 L volume) were converted to total C fluxes in the water column, assuming a water column of 10 m above the reef (i.e., 10 m³ of seawater per m² of reef). Outliers (i.e., values more than three interquartile ranges away from the 1st and 3rd quartiles of the sampled

population) were removed and the 95-percentile ranges of these total fluxes were entered in the model to constrain flows of planktonic, detrital, and dissolved organic C.

Hourly consumption and production rates of detrital and dissolved organic C by the sessile functional groups were determined from incubations of abundant species (see Table S3) of scleractinian corals, gorgonians, crustose coralline algae, non-calcifying algae, as well as rock and sediment communities (light: $n = 6-28$, dark: $n = 6-24$ per functional group; see Supplementary methods for details). Similarly, grazing rates on bacterio- and phytoplankton were determined during incubations of the sessile functional groups, based on the observed changes in plankton concentrations measured by flow cytometry. Calculations of the C fluxes by the sessile functional groups were corrected for significant C fluxes measured in incubations of unfiltered natural seawater without sessile organisms (Table S4), taking into account the seawater volume in the incubation chambers, and were standardized to organism abundances (expressed as g_{AFDW} , cm^3 , or cm^2 , depending on the functional group, see Table 1). Subsequently, we calculated 95-percentile ranges of the C flows measured in the replicate incubations assuming a normal distribution of the data.

Primary productivity & respiration

Daily metabolic rates of each phototrophic group were calculated using changes in irradiance during daylight to account for hourly variation of photosynthesis and respiration rates (Figure S1; Odum and Odum 1955; Fang et al. 2013). Fluxes of O_2 were measured using continuous data logging every 60 s to estimate net primary productivity (NPP_h) and nighttime respiration rates (R_n), expressed per hour, from light and dark incubations. Measurements were converted from O_2 into C, assuming a photosynthetic quotient (i.e., mol O_2 produced per mol CO_2 assimilated) of 1.19 for light incubations and a respiratory quotient (i.e., mol CO_2 respired per mol O_2 consumed) of 0.93 for dark incubations (see Table S1 for references of assumed parameters). Daily respiration R was calculated as:

$$(1) \quad R = R_n (24 + 7.115 \cdot (F_R - 1)),$$

where F_R is a group-specific elevated daytime respiration factor (Table S1), assuming that respiration rises from R_n in the morning to $R_n \cdot F_R$ at midday, and back to R_n in the evening (Figure S1). The irradiance factor 7.115 captures the daily rise and fall of the photosynthetically active radiation (PAR), and was obtained by calculating the definite integral of the average PAR curve between 06:00 and 18:00 hours in the study area (PAR data available at power.larc.nasa.gov/data-access-viewer). Daily gross primary productivity GPP was calculated by multiplying the sum of NPP_h and respiration at midday with the same irradiance factor:

$$(2) \quad GPP = 7.115 (NPP_h + R_n \cdot F_R).$$

GPP by massive sponges was calculated using reported P:R ratios (rates expressed per hour, Table S1), because NPP rates were not available for sponges. The reported P:R ratios were based on GPP measured in the light divided by R measured in darkness. For consistency, these P:R ratios were also adjusted for elevated daytime respiration according to:

$$(3) \quad P:R_{\text{adjusted}} = \frac{(P:R_{\text{original}} + (F_R - 1))}{F_R}$$

The mean adjusted P:R ratio (i.e., 1.92) was then multiplied with respiration and integrated over the full daytime according to:

$$(4) \quad GPP = 7.115 \cdot R_n \cdot F_R \cdot 1.92 \cdot 0.3,$$

where the factor 0.3 reflects previous observations that ~30 % of Caribbean sponges contain photosymbionts (Wilkinson 1987; Diaz and Rützler 2001; Erwin and Thacker 2007). GPP by encrusting sponges was calculated similarly using reported P:R ratios (mean adjusted P:R = 0.96, n = 3). Another estimate for GPP by encrusting sponges was calculated from the recently estimated ratio between daily-integrated rates of GPP and R (0.24) reported in Hudspith et al. (2022) for *Chondrilla caribensis* (i.e., $GPP = R \cdot 0.24 \cdot 0.3$).

Daily respiration rates of non-phototrophic groups (motile invertebrates and fish) were estimated by multiplying previously reported rates of respiration, expressed per hour, by 24 h, using specific respiratory quotients of 0.75 for motile invertebrates (Hatcher 1989) and 0.73 for fish (Price and Mager 2020) to convert O₂ into CO₂.

Motile consumers & dissolution of detritus

Total rates of grazing, predation, and detritus production by motile invertebrates and fishes (PLG, AG, PR, and DP of motile consumers in Box 1) were obtained from the published literature (Table S1). Wet weights reported for their tissues and feces were converted to organic C using available conversion factors (Stickney and Torres 1989; Brey et al. 2010). To estimate C uptake from grazing on plankton and non-calcifying algae and predation, the total consumption rates by motile invertebrates and fish reported in existing trophic models of Caribbean coral reefs (Opitz 1993; Cáceres et al. 2016) were partitioned into different food sources using the diet composition matrices reported in Opitz (1993), assuming that half of the reported “sessile animals” are corals and the other half sponges. These C fluxes were constrained in the model using the smallest and largest values extracted from Opitz (1993) and Cáceres et al. (2016) as minima and maxima, respectively.

Finally, minimum and maximum rates of dissolution of detritus into dissolved organic C were calculated as 54 % of the minimum and 80 % of the maximum (percentages taken from Wild et al. 2004a) combined detritus production by scleractinian corals and gorgonians as determined from the *in-situ* incubations.

Inflow and outflow at the model boundaries

Most of the dissolved and particulate C transported by the ocean currents above a square meter of reef is not processed by the reef community and instead simply passes over the reef (i.e., “throughflow”, Figure 1). Throughflows (TF) of plankton, detritus, and dissolved C were each calculated as:

$$(5) \quad TF_x = v_{wc} \cdot c_x \cdot a,$$

where the index x refers to either plankton, detritus, or dissolved organic C, v_{wc} is the average current velocity (0.115 m s^{-1}) at 10 m depth at our study site (van Duyl et al. 2006), c_x is the average organic C concentration (in mmol C L^{-1}) of plankton, detritus, or dissolved organic C in the water column, and the factor a ($= 864,000,000$) integrates the flux over the 10 m water column and converts the units $\text{m}^3 \text{ s}^{-1}$ to L d^{-1} . The concentrations of c_x were quantified in samples of reef water (at 0.1–5 m above the reef), open ocean water (1 km offshore at 1.5 m water depth) and of all reef water sampled at $t = 0$ from our *in-situ* incubations ($n = 139, 133, \text{ and } 212$ for plankton, detritus, and dissolved C, respectively).

The total inflow of organic carbon (IN in Box 1) into our model space is defined as the throughflow plus the organic C imported by the reef community (IMP), where IMP can vary between zero (i.e., no external C is consumed by the reef community) and an estimated maximum. Imported planktonic, detrital, and dissolved organic C thus represents the part of the total C inflows that is incorporated into the reef community. Maximum imports of C into the reef community were estimated by summing (i) the maximum possible amount of plankton, detritus, and dissolved organic C entering the diffusive boundary layer (DBL), (ii) the transfer of open ocean organic C to the reef benthos via active pumping by filter feeders (FF), which is not limited by diffusion in the DBL, and (iii) uptake of C by the planktonic community within the water column (pl):

$$(6) \quad IMP_{\max} = IMP_{\text{DBL}} + IMP_{\text{FF}} + IMP_{\text{pl}}.$$

Maximum mass transfers of plankton, detritus, and dissolved C within the DBL were each estimated as:

$$(7) \quad IMP_{\text{DBL}} = 0.5 Q \cdot c_x^*,$$

where Q is the maximum seawater volume flow (in $\text{L m}^{-2} \text{ d}^{-1}$) within the DBL and c_x^* is the 97.5-percentile of the planktonic, detrital, or dissolved C concentration (in mmol C L^{-1}) measured in the open ocean ($n = 15$). The factor 0.5 assumes a linear concentration gradient from c_x^* at the top to zero at the bottom of the DBL due to benthic uptake of C (Patterson 1992a; Falter et al. 2016). To limit imports of dissolved C to its labile components, the right side of Equation (7) was multiplied with 0.2 (de Goeij and van Duyl 2007) when c_x^* refers to dissolved organic C. Maximum volume flow was calculated as:

$$(8) \quad Q = h \cdot v_{\text{DBL}} \cdot fr \cdot 86.4,$$

assuming a DBL height $h = 0.12$ cm thickness, a maximum seawater flow velocity $v_{DBL} = 1.8$ cm s^{-1} within the DBL, and a mean rugosity $fr = 271$ cm m^{-2} (see Table S1 for the references), while the factor 86.4 converts $cm^3 m^{-2} s^{-1}$ to $L m^{-2} d^{-1}$.

Maximum rates of import of plankton, detritus, and dissolved organic C via filter feeding organisms, IMP_{FF} , were approximated using the 97.5-percentiles of the combined clearance rates determined for encrusting and massive sponges, which accounted for most of the filter feeder biomass and more than half of the total community biomass on the studied reef (Kornder et al. 2021). Finally, IMP_{pl} was approximated as the 97.5-percentile of the estimated total rates of C uptake by plankton.

The total outflow (OUT in Box 1) of organic carbon leaving the model space is defined as the throughflow plus organic C exported by the reef community (EXP), where EXP can vary between zero (i.e., no C produced by the reef community is exported) and an estimated maximum. Maximum export rates of planktonic, detrital, and dissolved organic C out of the reef community were calculated in the same way as their maximum import rates (i.e., $EXP_{max} = EXP_{DBL} + EXP_{FF} + EXP_{pl}$). However, in Equation (7) the term c_x^* was set as the 97.5-percentile of the planktonic, detrital, or dissolved C concentration measured above the reef ($n = 21$) and the 0.5 factor was removed to estimate EXP_{DBL} because we do not assume a steep concentration gradient of the exported C within the DBL. Further, EXP_{FF} and EXP_{pl} were estimated using the 97.5-percentiles of the release rates of C by sponges and plankton, respectively.

The mass balance equations of plankton, detritus, and dissolved organic C can be mathematically simplified. That is, the terms IN and OUT in the mass balances of the pelagic C pools:

$$(9) \quad \frac{dc_x}{dt} = IN_x + Production_x - Consumption_x - OUT_x$$

can be partitioned into their components (i.e., throughflow and imports/exports):

$$(10) \quad \frac{dc_x}{dt} = (TF_x + IMP_x) + Production_x - Consumption_x - (TF_x + EXP_x),$$

so that throughflow cancels out:

$$(11) \quad \frac{dc_x}{dt} = IMP_x + Production_x - Consumption_x - EXP_x.$$

This way, the model considers all organic C flowing into and out of the reef with the ocean current, but the mass balances of the reef are based only on the local excess C production or net C consumption and the import and export rates of organic C (i.e., IMP and EXP) by the local reef community. The inflow and outflow at the model boundaries and the estimated partitioning of the C fluxes are illustrated in Figure 1.

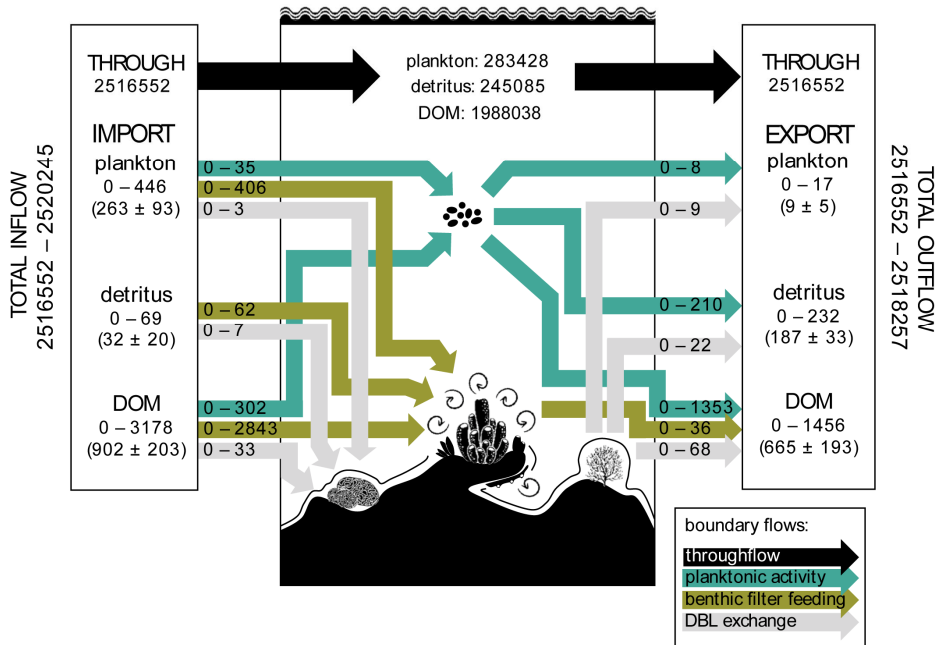


Figure 1. Design of the model highlighting inflows and outflows (in $\text{mmol C m}^{-2} \text{d}^{-1}$) of plankton, detritus, and dissolved organic matter (DOM). Total inflows and outflows of organic C were partitioned into C passing over the reef (throughflow, black arrows) and C that is imported and exported into and from the reef community. Ranges indicate possible import and export rates, where maxima were estimated by summing maximum net C fluxes by plankton (blue-green arrows), maximum filter feeding and excretion rates by sponges (brown arrows), and maximum transfer of C to and from the benthic community through the diffusive boundary layer (DBL, light gray arrows). Numbers in parentheses are statistical summaries (mean \pm SD) of the model solutions for these flows. All flows describing internal cycling of organic C within the reef community are depicted in Figures 2, 3 and Table S5.

Table 1. *In-situ* measured fluxes of organic carbon (C) normalized to tissue surface area (in cm²), biovolume (in cm³), or biomass (in g_{AFDW}) of incubated specimens. The 95-percentile ranges were used to constrain fluxes. Shaded values were obtained from dark incubations at sunrise, other values were measured in the light at midday. AFDW, ash-free dry weight; SW, seawater; n, sample size. Incubated taxa, biomass conversions, and specific sample sizes are listed in Table S3. Raw measurements are given in Supplementary data S1 (C fluxes) and S2 (O₂ fluxes).

group	mean	SD	95-percentiles		unit	n
			lower	upper		
net primary productivity (NPP_n)						
scleractinian corals	1.5177	0.9212	0.2499	3.4163	μmol C cm ⁻² h ⁻¹	27
gorgonians	7.8816	7.7072	1.1537	24.117	μmol C cm ⁻³ h ⁻¹	11
coralline algae	0.1574	0.1087	0.0260	0.2850	μmol C cm ⁻² h ⁻¹	6
non-calcifying phototrophs	297.58	185.40	102.17	697.87	μmol C g _{AFDW} ⁻¹ h ⁻¹	14
coral rock communities	1.1677	1.9808	-0.3222	4.5566	μmol C cm ⁻² h ⁻¹	6
cryptic rock communities	-0.0909	0.1189	-0.2214	0.0524	μmol C cm ⁻² h ⁻¹	6
sediment communities	0.1728	0.1289	-0.0190	0.2777	μmol C cm ⁻² h ⁻¹	5
plankton	-0.0654	0.2045	-0.4093	0.2269	μmol C L _{SW} ⁻¹ h ⁻¹	12
respiration (R_n)						
scleractinian corals	-0.8536	0.5109	-1.9408	-0.1774	μmol C cm ⁻² h ⁻¹	24
gorgonians	-5.7825	6.4155	-20.326	-0.9424	μmol C cm ⁻³ h ⁻¹	12
coralline algae	-0.0583	0.0209	-0.0896	-0.0386	μmol C cm ⁻² h ⁻¹	5
non-calcifying phototrophs	-80.366	46.540	-166.16	-35.373	μmol C g _{AFDW} ⁻¹ h ⁻¹	12
coral rock communities	-0.7145	0.2816	-1.1352	-0.3816	μmol C cm ⁻² h ⁻¹	6
cryptic rock communities	-0.1954	0.1125	-0.3375	-0.1097	μmol C cm ⁻² h ⁻¹	6
sediment communities	-0.2321	0.0402	-0.2693	-0.1931	μmol C cm ⁻² h ⁻¹	3
plankton	-0.1015	0.2413	-0.4757	-0.0126	μmol C L _{SW} ⁻¹ h ⁻¹	7
net DOM production (+) or DOM consumption (-)						
scleractinian corals	0.1596	0.1986	-0.1146	0.6274	μmol C cm ⁻² h ⁻¹	24
	0.2550	0.1831	-0.0085	0.5842	μmol C cm ⁻² h ⁻¹	22
gorgonians	3.1968	2.1551	0.7512	7.0308	μmol C cm ⁻³ h ⁻¹	9
	2.3426	3.2139	0.5126	9.5566	μmol C cm ⁻³ h ⁻¹	11
coralline algae	0.0107	0.0205	-0.0162	0.0314	μmol C cm ⁻² h ⁻¹	7
	0.0141	0.0108	0.0041	0.0318	μmol C cm ⁻² h ⁻¹	6
non-calcifying phototrophs	37.504	53.210	-7.1059	170.46	μmol C g _{AFDW} ⁻¹ h ⁻¹	17
	41.850	32.621	5.7761	99.660	μmol C g _{AFDW} ⁻¹ h ⁻¹	13
coral rock communities	0.1695	0.1082	0.0697	0.3081	μmol C cm ⁻² h ⁻¹	4
	0.1391	0.1832	-0.0905	0.4161	μmol C cm ⁻² h ⁻¹	6
cryptic rock communities	0.0865	0.0999	-0.0358	0.2337	μmol C cm ⁻² h ⁻¹	6
	0.0416	0.0287	0.0165	0.0821	μmol C cm ⁻² h ⁻¹	5
Sediment communities	0.0522	0.0572	-0.0407	0.1096	μmol C cm ⁻² h ⁻¹	6
	0.0562	0.0474	0.0031	0.1204	μmol C cm ⁻² h ⁻¹	6
plankton	2.8078	2.1158	-1.2582	5.5418	μmol C L _{SW} ⁻¹ h ⁻¹	11
	1.8381	2.3544	-1.2600	5.7297	μmol C L _{SW} ⁻¹ h ⁻¹	12
net detritus production (+) or detritus consumption (-)						
scleractinian corals	0.1628	0.1495	0.0048	0.4964	μmol C cm ⁻² h ⁻¹	23
	0.2175	0.2681	-0.0151	0.7900	μmol C cm ⁻² h ⁻¹	18
gorgonians	1.0810	0.5279	0.3529	1.9262	μmol C cm ⁻³ h ⁻¹	11
	0.6744	1.1013	-0.1168	3.1412	μmol C cm ⁻³ h ⁻¹	11
coralline algae	0.0158	0.0191	0.0036	0.0515	μmol C cm ⁻² h ⁻¹	7
	0.0088	0.0114	0.0011	0.0300	μmol C cm ⁻² h ⁻¹	7

group	mean	SD	95-percentiles		unit	n
			lower	upper		
coral rock communities	0.0544	0.0483	0.0102	0.1136	$\mu\text{mol C cm}^{-2} \text{ h}^{-1}$	6
	0.0646	0.0502	0.0146	0.1353	$\mu\text{mol C cm}^{-2} \text{ h}^{-1}$	6
cryptic rock communities	0.0213	0.0313	-0.0004	0.0748	$\mu\text{mol C cm}^{-2} \text{ h}^{-1}$	6
	0.0003	0.0003	0.0000	0.0006	$\mu\text{mol C cm}^{-2} \text{ h}^{-1}$	6
plankton	0.3147	0.4310	-0.1540	1.0517	$\mu\text{mol C L}_{\text{sw}}^{-1} \text{ h}^{-1}$	7
	0.2379	0.2947	-0.0799	0.6939	$\mu\text{mol C L}_{\text{sw}}^{-1} \text{ h}^{-1}$	8
net plankton production (+) or plankton consumption (-)						
scleractinian corals	-0.0019	0.0092	-0.0244	0.0085	$\mu\text{mol C cm}^{-2} \text{ h}^{-1}$	27
	-0.0015	0.0089	-0.0146	0.0154	$\mu\text{mol C cm}^{-2} \text{ h}^{-1}$	19
gorgonians	0.0292	0.0387	-0.0132	0.0907	$\mu\text{mol C cm}^{-3} \text{ h}^{-1}$	10
	-0.0382	0.0586	-0.1653	0.0095	$\mu\text{mol C cm}^{-3} \text{ h}^{-1}$	11
coral rock communities	-0.0009	0.0037	-0.0049	0.0039	$\mu\text{mol C cm}^{-2} \text{ h}^{-1}$	6
	-0.0070	0.0041	-0.0112	-0.0012	$\mu\text{mol C cm}^{-2} \text{ h}^{-1}$	6
cryptic rock communities	-0.0001	0.0037	-0.0054	0.0049	$\mu\text{mol C cm}^{-2} \text{ h}^{-1}$	6
	-0.0026	0.0025	-0.0055	0.0009	$\mu\text{mol C cm}^{-2} \text{ h}^{-1}$	6
sediment communities	0.0003	0.0021	-0.0018	0.0034	$\mu\text{mol C cm}^{-2} \text{ h}^{-1}$	6
	-0.0003	0.0018	-0.0028	0.0008	$\mu\text{mol C cm}^{-2} \text{ h}^{-1}$	5
plankton	-0.0810	0.0533	-0.1642	0.0035	$\mu\text{mol C L}_{\text{sw}}^{-1} \text{ h}^{-1}$	11
	-0.0187	0.0638	-0.1244	0.0667	$\mu\text{mol C L}_{\text{sw}}^{-1} \text{ h}^{-1}$	8

RESULTS & DISCUSSION

We present a carbon flow model (Box 1) of the food web of a Southern Caribbean coral reef based on 192 *in situ* incubations of primary productivity and respiration rates as well as net planktonic, detrital, and dissolved organic C uptake and release rates by common benthic reef organisms (Table 1). We combined these field data with additional C fluxes, metabolic ratios, biomass data, and hydrodynamic parameters from 76 publications (Table S1).

Organic C in the water column above the reef consisted mostly of dissolved organic C (79%), with smaller contributions by plankton (11%) and detritus (10%). The amount of dissolved and suspended organic C in the water column is minor in comparison to the amount of organic carbon stored in the benthic reef community (Figure 2A). However, due to the current velocities above the reef (van Duyl et al. 2006), the model predicts that the total organic C transported within the water column above the reef ($2517 \text{ mol C m}^{-2} \text{ d}^{-1}$) was three orders of magnitude larger than the combined metabolic fluxes of all reef organisms ($5290 \text{ mmol C m}^{-2} \text{ d}^{-1}$). This pattern illustrates that reefs inhabiting oligotrophic waters can still be supplied with relatively large amounts of allochthonous carbon by the currents. Yet only a small fraction of this large pelagic carbon flow is imported by the reef community (Figure 1). This is mainly due to the formation of boundary layers and physical and biological constraints (e.g., diffusion, rates of phago- or pinocytosis), limiting the amount of organic carbon actually taken up by the benthic community (Patterson 1992b; Shashar et al. 1996). Plankton was net imported by the benthic reef community, import and export of dissolved organic C

were of similar magnitude, whereas detritus was largely net exported by the reef (Figure 1). In total, gross import of allochthonous C ($1196 \pm 202 \text{ mmol C m}^{-2} \text{ d}^{-1}$, mean \pm SD throughout text) exceeded gross export ($860 \pm 197 \text{ mmol C m}^{-2} \text{ d}^{-1}$), pointing towards net uptake of organic C by the reef from the ocean water. Unfortunately, in the current LIM, the origin of allochthonous organic carbon (e.g., terrestrial or oceanic) could not be determined. However, this information can be added to future LIMs by using data from, for example, stable isotope mixing models (van Duyl et al. 2011; Carreón-Palau et al. 2013).

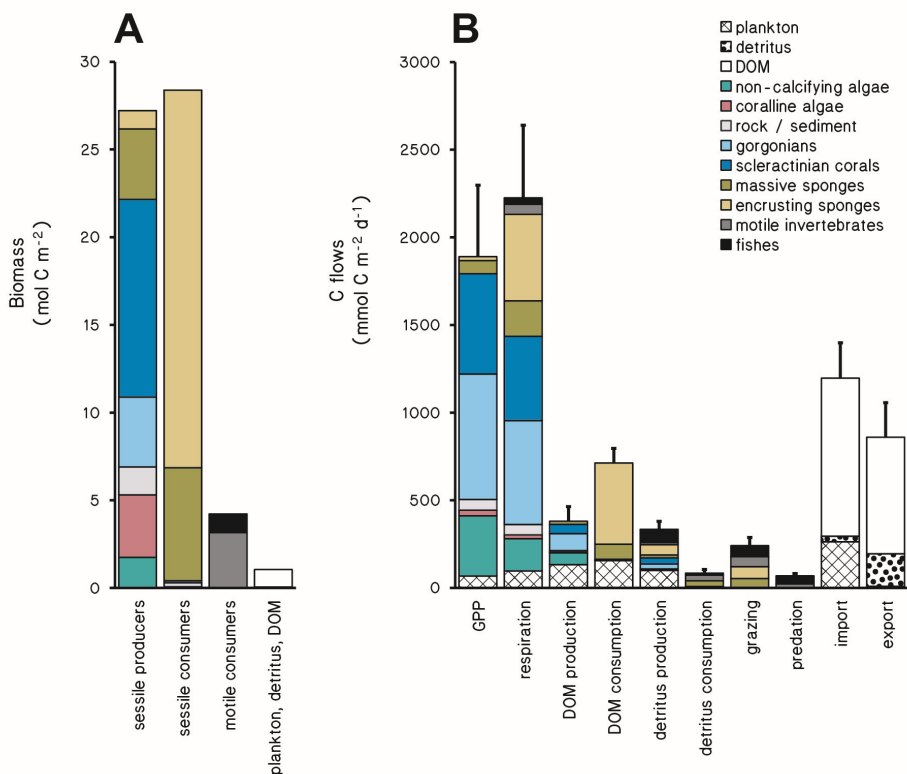


Figure 2. Carbon storage and flows of a Caribbean coral reef. **(A)** Mean standing biomass (in mol C m^{-2}) on the reef slope (9–14 m depth) along the leeward shore of Curaçao, partitioned among the different functional groups and their role in the food web. **(B)** Predicted mean C flows (in $\text{mmol C m}^{-2} \text{ d}^{-1}$) on the same reef, partitioned by the contributions of the different functional groups to each process. Error bars are SDs of totals. “Grazing” in (B) combines grazing on macroalgae and plankton, by each of the indicated consumers (sponges, motile invertebrates and fish). GPP, gross primary productivity; DOM, dissolved organic matter.

Overall, the GPP of the reef community averaged $1890 \pm 408 \text{ mmol C m}^{-2} \text{ d}^{-1}$ (Figure 2B). Community respiration ($R = 2226 \pm 414 \text{ mmol C m}^{-2} \text{ d}^{-1}$) exceeded GPP, suggesting that the reef community is net heterotrophic (P:R ratio = 0.84 ± 0.05) and net import of allochthonous C supplemented the ecosystem's respiratory demand (Figure 2B). Furthermore, we estimated that consumer biomass (i.e., the biomass of heterotrophic groups) slightly exceeded producer biomass in this reef community (Figure 2A).

Within the reef community, a large fraction of the GPP by non-calcifying algae (20 %), scleractinian corals (9 %) and gorgonians (13 %) was released as dissolved organic C, while the GPP by non-calcifying algae was additionally grazed by herbivorous fishes (18 %) and motile invertebrates (17 %) (Figures 2, 3, Table S5). Both sponges and plankton (including bacterio- and phytoplankton) consumed substantial amounts of dissolved organic C (29 % and 8 % of total community GPP, respectively). Reef community detritus production ($343 \text{ mmol C m}^{-2} \text{ d}^{-1}$) was similar to the community production of dissolved organic C ($380 \text{ mmol C m}^{-2} \text{ d}^{-1}$). Detritus was largely produced by plankton, fish, and sponges (30 %, 22 %, 22 % of total detritus production, respectively) (Figures 2, 3, Table S5). A large part of the detritus production was exported from the reef ($187 \text{ mmol C m}^{-2} \text{ d}^{-1}$) and the remaining part was processed by organisms residing on the reef, particularly massive sponges and motile invertebrates.

The internal carbon flows were generally well-constrained by the model. The coefficients of variation for individual C flows were $43 \pm 19 \%$, and did not exceed 85 % (Figure S2), which is comparable to the coefficients of variation in other LIMs (Kones et al. 2009; van Oevelen et al. 2009). Below, we discuss our model outcomes and highlight several limitations of our LIM.

High primary productivity of Caribbean reefs

The community GPP from this study ranks among the highest obtained for coral reefs (Table 2). The GPP of a variety of tropical shallow-water coral reef ecosystems was estimated several decades ago, and typically ranged between 200 and $500 \text{ mmol C m}^{-2} \text{ d}^{-1}$ (Kinsey 1983; Kinsey 1985; Hatcher 1988), although it was then already acknowledged that Caribbean coral reefs can be distinctively more productive (Hatcher 1990). In fact, our modeled estimates are comparable to GPP rates determined 40 years ago for similar Caribbean reefs ($1416\text{--}2890 \text{ mmol C m}^{-2} \text{ d}^{-1}$) (Wanders 1976; Adey and Steneck 1985). The model thus corroborates that coral reefs of the Caribbean are more productive than their Indo-Pacific counterparts (Atkinson and Grigg 1984; Kinsey 1985; Johnson et al. 1995; Gattuso et al. 1996; Hata et al. 2002). Whether the GPP of reefs in other geographical areas has changed compared to values established decades ago is unknown, as recent estimates of reef GPP are lacking.

Table 2. Estimates of gross community primary productivity (GPP) of coral reefs through six decades.

region	GPP [mmol C m ⁻² d ⁻¹]	source
Caribbean	2889*	(Wanders 1976)
Global	68–1141	(Lewis 1977)
Indo-Pacific	333–1582	(Kinsey 1983; Kinsey 1985)
Indo-Pacific	83–1666	(Atkinson and Grigg 1984)
Caribbean	1416–2749	(Adey and Steneck 1985)
Caribbean	167–583	(Hatcher 1988,1990)
Caribbean	416–1666	(Sorokin 1990)
Indo-Pacific	1324	(Johnson et al. 1995)
Indo-Pacific	750–1249	(Gattuso et al. 1996)
Indo-Pacific	599–675	(Hata et al. 2002)
Caribbean	1177–2599	This study

*measured in very shallow reefs (0.5–3 m water depth)

On average, we found that gorgonians, scleractinian corals, and non-calcifying algae accounted for respectively $38 \pm 17 \%$, $30 \pm 11 \%$ and $19 \pm 5 \%$ of the total community's GPP (Figure 2B). However, non-calcifying algae and gorgonians were more productive than scleractinian corals when GPP was related to their biomass (1.9 mol C m^{-2} (algae), 4.0 mol C m^{-2} (gorgonians), and $11.5 \text{ mol C m}^{-2}$ (scleractinian corals), Figure 2A, biomass data from Kornder et al. 2021). The primary productivity of reefs can thus increase following coral-algal phase shifts (Kayanne et al. 2005; Roth 2019), although patterns of algal community composition and productivity are strongly influenced by local herbivory and nutrient loads (Done 1992; Lapointe et al. 1997; Littler et al. 2006). Locally, some reef sites on Curaçao showed a shift in primary producing communities over the past decades, as corals were increasingly replaced by non-calcifying algae, such as macroalgae and benthic cyanobacterial mats (de Bakker et al. 2017). However, in light of the historic estimates of GPP by Caribbean reef communities (Table 2), our estimate for the present-day reef community on Curaçao is indicative of rather stable GPP throughout recent decades, despite observed changes in community composition.

The total community biomass represented 8 % of its estimated annual GPP, meaning a turnover of its standing biomass C stock in approximately one month. The turnover time, or its inverse (i.e., turnover rate), is commonly used in assessments of ecosystem functions including biomass storage and flows on coral reefs (Christensen 1995; Cheng et al. 2009; Liu et al. 2009; Ainsworth and Mumby 2015; Schramski et al. 2015; Argüelles-Jiménez et al. 2021; Calderon-Aguilera et al. 2021). Interestingly, the turnover time of biomass on coral reefs across both the Indo-Pacific and the Caribbean region appears very consistent at $8 \pm 2 \%$ of their annual GPP ($n = 12$, Figure 3), despite geographical differences in their ecology and profound differences in methodologies to estimate biomass and productivity across these studies.

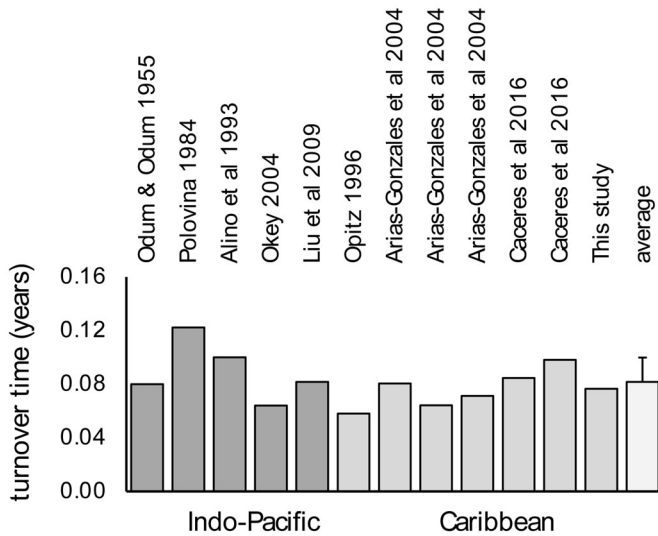


Figure 3. Estimated turnover time (ratio between standing biomass and annual gross primary productivity, in years) for various Indo-Pacific (dark grey bars) and Caribbean (light grey bars) coral reefs. White bar on far right is the average (\pm SD) across all reefs.

Net heterotrophy despite high primary productivity

Daily rates of total community respiration exceeded GPP (Figure 2B), making the system net heterotrophic with a negative net primary productivity (NPP) of 337 ± 86 mmol C m⁻² d⁻¹ (Table S5). Excess respiration was counterbalanced by allochthonous organic C imports, which accounted for 39 ± 6 % of the total C input (i.e., sum of C import and GPP) (Figures 2, 3, Table S5). Our result corroborates recent *in-situ* measurements of GPP over 24 h on the reefs studied here, and on the neighboring island of Bonaire, showing that benthic reef communities respired more C than they fixed (van Heuven et al. 2018; Webb et al. 2021). In addition, the potential for allochthonous subsidies driving trophodynamics on coral reefs is increasingly recognized (Sorokin and Sorokin 2010; Davis et al. 2014; Skinner et al. 2021). Together, these findings may indicate that the community metabolism of reefs has shifted from being in net balance (P:R = 1) or net autotrophic a few decades ago to being net heterotrophic at present. In other words, where coral reefs were historically considered to be self-sufficient in oligotrophic tropical waters (Odum and Odum 1955; Glynn 1973; Wanders 1976; Adey and Steneck 1985; Hatcher 1988,1990), future reefs may develop communities that are increasingly dependent on net import of external organic matter (Birkeland 2015). In this study, the net import of organic C consisted of plankton (254 ± 93 mmol C m⁻² d⁻¹) and DOM (237 ± 79 mmol C m⁻² d⁻¹; Figure 1). Encrusting sponges, generally “overlooked” in resource cycling and community composition assessments, accounted foremost for the observed net heterotrophy on present-day coral reefs (and possibly already on reefs in the past) through their significant contribution to the community’s total respiratory demand, DOM consumption, and

plankton grazing rates (Figures 2, 3, Table S5). Unfortunately, we cannot compare their present-day carbon fluxes to their historic (i.e., pre-2000) contribution to carbon cycling.

Internal C flows are dominated by benthic-pelagic coupling

Most of the C transfer among reef organisms occurred via the DOM and detritus pool ($1512 \text{ mmol C m}^{-2} \text{ d}^{-1}$, total combined dissolved organic C and detrital C production and consumption rates; Figure 4, Table S5). Grazing on plankton and non-calcifying algae ($241 \pm 47 \text{ mmol C m}^{-2} \text{ d}^{-1}$) and predation ($69 \pm 12 \text{ mmol C m}^{-2} \text{ d}^{-1}$) represented much lower C flows. In total, grazing on plankton and non-calcifying algae represented 13 % of the community GPP, whereas 22 ± 8 % of GPP was released as DOM ($381 \pm 83 \text{ C m}^{-2} \text{ d}^{-1}$), mainly by corals and gorgonians (40 ± 13 % of total DOM production), but also by plankton (34 ± 14 %) and macroalgae (18 ± 10 %) (Figure 2B). The largest DOM consumption was by sponges ($549 \pm 57 \text{ mmol C m}^{-2} \text{ d}^{-1}$) and plankton ($156 \pm 77 \text{ mmol C m}^{-2} \text{ d}^{-1}$). Total DOM consumption of the reef community thus exceeded its DOM production, which rendered the reef a sink of DOM (net community uptake: $237 \pm 79 \text{ mmol C m}^{-2} \text{ d}^{-1}$). Previous studies have shown that sponges use DOM (de Goeij et al. 2008b; Campana et al. 2021) to satisfy their minimal respiratory demands (total R by encrusting and massive sponges was $696 \pm 85 \text{ mmol C m}^{-2} \text{ d}^{-1}$). Within the plankton community, DOM is mainly utilized by heterotrophic bacteria. At our study site, 60 % of the measured plankton consisted of heterotrophic bacteria, and grazing on these bacteria accounted for 54 % of the total grazing on plankton by benthic organisms (Figure S3). Based on these percentages, the amount of DOM that enters the detritus food chain as sponge waste ($74 \pm 27 \text{ mmol C m}^{-2} \text{ d}^{-1}$) was comparable to the total grazing rate on bacterioplankton ($89 \pm 24 \text{ mmol C m}^{-2} \text{ d}^{-1}$). This suggests that the sponge loop (de Goeij et al. 2013) and microbial loop (Azam et al. 1983) contributed similarly to the retention of the locally produced DOM that would otherwise have been lost from the reef system.

Sponge waste and other sources of detritus (coral mucus: $64 \pm 29 \text{ mmol C m}^{-2} \text{ d}^{-1}$; fish feces: $75 \pm 24 \text{ mmol C m}^{-2} \text{ d}^{-1}$) exceeded total detritus consumption ($84 \pm 21 \text{ mmol C m}^{-2} \text{ d}^{-1}$), leading to an excess production of detritus on the reef, that was partly released into the water column (net export: $155 \pm 37 \text{ mmol C m}^{-2} \text{ d}^{-1}$) and partly dissolved into DOM ($96 \pm 29 \text{ mmol C m}^{-2} \text{ d}^{-1}$). Overall, our model estimated that the production and consumption of DOM and detritus are tightly coupled within the studied reef community. This corroborates the historically found efficient recycling of photosynthetically fixed C on coral reefs via a diverse heterotrophic community (Odum and Odum 1955; Kinsey 1983; Hatcher 1988).

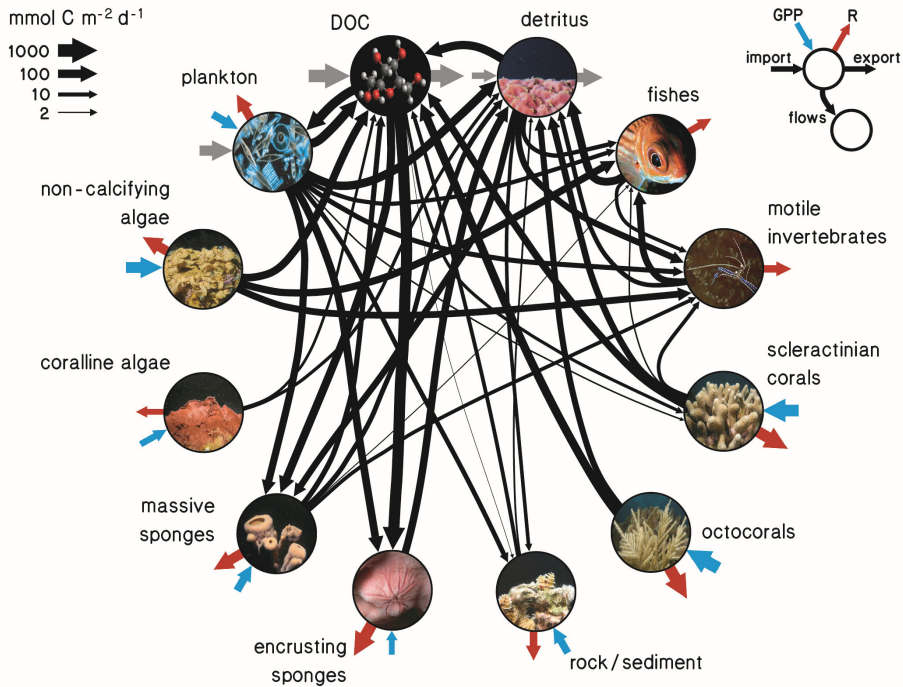


Figure 4. Carbon flows in the food web of a Caribbean coral reef. Arrow widths are natural logarithms of metabolic rates (blue arrows: gross primary productivity, red arrows: respiration), imports and exports of C (grey arrows), and C flows between compartments (black arrows); all C flows are in $\text{mmol C m}^{-2} \text{ d}^{-1}$. Marginal fluxes not shown include dissolved organic matter (DOM) uptake by non-calcifying algae, plankton grazing by gorgonians and rock/sediment communities, and detritus uptake by corals. A summary of all C flows and associated data sources is given in Table S5.

Limitations of the model

Four important assumptions underlie our model. First, the model assumes that reef communities are in steady state. This means that estimates of GPP and R may potentially be skewed towards parity by the balancing algorithm of the model (Allesina and Bondavalli 2003; Fath et al. 2007). If so, community R may exceed community GPP even more than suggested by the model. In addition, any processes that require excess C (e.g., growth of organic tissue, reproduction by e.g., coral spawning, immune defense) were not considered here. The analyses of Vézina and Pahlow (2003) indicate that the steady-state assumption introduces only limited bias in the model solutions of LIMs, primarily because net biomass increases (of the benthic and pelagic groups) are small compared to the other C flows in marine food webs. To investigate possible under- or overestimation of NPP due to the

assumption of dynamic equilibrium in coral reef communities, trophic models need to be evaluated against actual measurements of NPP in coral reef communities. A validation of our model predictions against several community C fluxes obtained *in situ* is presented in Chapter 5.

Second, the model assumes that respiration in benthic phototrophs increases during the day by up to 25-fold compared to night-time respiration (Figure S1; Table S1; Odum and Odum 1955; Adey and Steneck 1985; Fang et al. 2014; Schrammeyer et al. 2014). This assumption doubled our estimates of community GPP and R. Although we added extensive data on day versus night C flows for reef communities, enhancement of R in the light was based on a very limited set of data from the literature (Table S1). In particular, we found very few studies on diurnal variation in respiratory rates of reef organisms. Most likely, many C fluxes vary during 24 h day/night cycles, as has been revealed by studies demonstrating suppressed night-time release of mucus by corals (Crossland 1987) or enhanced night-time release of DOM by turf algae and benthic cyanobacterial mats (Mueller et al. 2022). More efforts should be made to incorporate diurnal variation in studies estimating daily respiration rates and fluxes of organic C by coral reef taxa.

Third, the model assumes that seawater pumping by filter-feeding animals creates a substantial water flow through these organism. This flow increases import and export rates of dissolved and particulate organic matter beyond the limited mass transfer within the diffusive boundary layer. In addition, net uptake or release of C by plankton that derives from or is consumed by benthic organisms also contributes to the reef community's import and export rates. These assumptions enabled the aforementioned import of allochthonous C, supplementing the ecosystem's respiratory demand. If pumping by filter feeders and net C fluxes by plankton were not considered, the net imports estimated by our model would be marginally small—that is, 99.999 % of all organic C passing above the reef would not be incorporated into the reef community—, and the modeled community P:R would approach one (Chapter 6). Conversely, consideration of the abovementioned additional C flows increased the imported fraction of all organic C passing above the reef from 0.001 to 0.050 % (i.e., the C flux into the reef benthic communities increased from 27 ± 9 to 1196 ± 202 mmol C m⁻² d⁻¹, Chapter 6), which is enough to sustain a community P:R ratio below one (Table S5). Our model thus illustrates how organic C uptake by filter feeders (e.g., the sponge loop) and plankton (microbial loop) can represent important subsidies of allochthonous C that contribute to the maintenance of net heterotrophy in coral reef communities (Birkeland 2015). Additional inputs of C may also come from terrestrial runoff or groundwater intrusion. While such inputs may be small in the studied area (M.J.A. Vermeij, personal communication), land-based subsidies of organic material should be considered in areas where they may represent a

significant source of C to reef communities (Suzuki and Kawahata 2003; Webb et al. 2019; Luijendijk et al. 2020).

Fourth, the model assumes that 30 % of the sponges on the reef supplement their C diet through photoautotrophy (Wilkinson 1987; Diaz and Rützler 2001; Erwin and Thacker 2007; Thacker et al. 2007; Erwin and Thacker 2008a,b; Pawlik et al. 2015; Bell et al. 2020; Freeman et al. 2021). The primary productivity of these sponges was constrained using published P:R ratios ranging from 0.43 (Freeman et al. 2013) to 5.0 (Thacker et al. 2007) ($n = 12$, Table S1). A lot is still unknown about photosynthesis in sponges. However, even the encrusting sponge *Chondrilla caribensis* living in low-light cryptic habitats can supplement its heterotrophic diet via photosynthesis (daily P:R = 0.24) (Hudspith et al. 2022). The high abundance of sponges on Caribbean coral reefs (Lesser and Slattery 2018; Pawlik and McMurray 2020; Kornder et al. 2021), including several taxa hosting photosymbionts, suggests that their potential contribution to community GPP is undervalued in coral reef ecology.

In addition to the above-mentioned assumptions, we note that C fluxes mediated by motile and endolithic fauna, as well as free-living and symbiotic bacteria, were poorly resolved by our model. The contributions by motile invertebrates and reef fishes were constrained on the basis of reported wet weights, conversions thereof into C, and diet composition matrices (Table S1). Cryptobenthic fishes (Brandl et al. 2018) could not be reliably quantified, as no comparative studies of their biomasses and C flows were available. Furthermore, endolithic taxa live deep inside the calcium carbonate rock (Odum and Odum 1955; Diaz and Rützler 2001) and were likely underrepresented by the dm^3 -sized fragments in our *in-situ* incubations. Grazing rates on plankton and non-calcifying algae as well as predatory C fluxes to higher-level consumers could therefore be higher than suggested by our model analysis. Finally, while symbiotic bacteria are implicitly incorporated in other functional groups, such as sponges and corals, in accordance with our approach of assessing these groups as holobionts, further studies will be essential to quantify the contributions of free-living benthic bacteria to the reef's C cycle.

Finally, we stress that our carbon flow model explicitly considers organic C, while reef communities grow in height due to the accretion of inorganic calcium carbonate. The LIM presented here can therefore not be used to estimate the balance between reef accretion and erosion, or to estimate how interactions in the food webs affect marine calcification. Integrating the inorganic and organic carbon flows on coral reefs (e.g., Diaz-Pulido and Barrón 2020; Tansik et al. 2021), including calcification and dissolution of carbonate rock, represents a crucial next step, as calcification of corals and coralline algae is hampered by ocean acidification

and global warming (Eyre et al. 2018; Perry and Alvarez-Filip 2019; Cornwall et al. 2021).

Conclusions

In summary, our model describes a coral reef community characterized by net heterotrophy despite very high rates of community GPP. Allochthonous plankton and DOM supplemented the system's respiratory demand, while the biomass of primary producers was slightly lower than total consumer biomass. Together, the community's organic carbon biomass was equal to ~8 % of the local annual GPP. Despite an increase of macroalgae, turf algae and benthic cyanobacterial mats in Caribbean reef communities since the 1970s (Roff and Mumby 2012), including the reefs studied here (de Bakker et al. 2017), a network of C fluxes in grazing and detrital food chains maintained a diverse range of trophic connections. Internal C fluxes were dominated by the transformation of dissolved coral and algal photosynthates into detritus via the sponge and microbial loops. Poorly resolved aspects that would benefit from additional empirical investigation include photoautotrophy and detritus production in sponges, diurnal variation in respiratory demands of phototrophic taxa, and the C flows mediated by motile animals and free-living bacteria on the reef. *In-situ* assessments of the C flows in other reef communities with a different taxonomic composition are also needed to validate predictions of our trophic framework. We hope our results will aid in developing comprehensive benchmarks of the biomass and C flows on modern coral reefs, to better understand and predict how carbon will be processed and stored in coral reef communities of the future.

Acknowledgements

We thank Eva de Rijke, Jorien Schoorl, and Rutger van Haal for their support with laboratory analyses. We also thank Benjamin Mueller, Beatrix Pereira and the Carmabi Research Foundation for their support with fieldwork activities. This work was funded by the European Research Council under the European Union's Horizon 2020 research and innovation programme (ERC Starting Grant agreement # 715513 to JMdG).

SUPPLEMENTARY INFORMATION

Supplementary methods

Organism collection & acclimatization

Data collection for this study was done at the Caribbean Research and Management of Biodiversity (Carmabi) field station on the island of Curaçao (12°12'N, 68°56'W) during four fieldwork seasons in 2019 (March/April, November/December) and 2020 (February/March, November/December). Local species and communities were selected for incubations based on island-wide biomass estimates (Kornder et al. 2021) to best represent each common benthic group (Table S3). Organisms were collected using SCUBA at 5–15 m water depth on the leeward fringing reefs in front of Carmabi and neighboring reefs. Whole coral colonies were collected whenever possible using a dive knife. Some fragments of massive corals were chiseled off the edge of larger colonies. All coral fragments were cleared off epibionts and kept on an artificial structure at 10 m depth to recover for at least one week. The structure was left on the reef to condition for four weeks prior to collections and consisted of PVC pipes and plastic bowls, anchored by a rope, and lifted into the water column by four air-filled 1-gallon containers. Gorgonians were collected whole by breaking off the rock at the base of the colony. Individuals were fixed onto small pieces of smooth dolerite rock (free of endobionts) to act as a new base using marine grade epoxy. The rocks themselves were then attached to the reef close to the incubation site using a small amount of additional epoxy, which could later be detached, to let gorgonians recover for at least one week. Macroalgae were collected haphazardly around the incubation site and gently shaken to remove loose epibionts prior to incubating. Small pieces of rubble fully covered in crustose coralline algae were collected by hand and placed into a preconditioned and weighted plastic box close to the incubation site to rest for at least three days. The box was designed to provide shelter and mimic light levels typically found in local cryptic reef habitats ($<20 \mu\text{mol photons m}^{-2} \text{s}^{-1}$, tested using HOBO Pendant UA-002-08 light logger, Onset, USA, spectral detection range: 150–1200 nm). To include inconspicuous reef communities, additional fragments of coral rock were collected from exposed and cryptic reef surfaces. Exposed rock fragments were kept next to coral fragments and contained primarily endolithic algae, excavating sponges, and polychaetes. Cryptic fragments were kept in the same sheltered boxes as coralline algae, and predominantly harbored bivalves, bryozoans, hydrozoans, and tunicates. Fragments were left to recover for at least three days prior to incubating. After recovery, all collected specimen were photographed from three angles (top, front, and side) next to a scale and their surface areas and volumes were estimated using delineation in ImageJ (version 1.X) (Schneider et al. 2012).

In-situ incubations & seawater sampling

A total of 192 *in-situ* incubations were performed in front of the Carmabi station at 10 m depth on the reef. Control incubations (n = 32) containing only seawater were performed periodically alongside incubations containing reef fauna. Some control incubations (n = 12) contained only the dolerite/epoxy bases used to stabilize gorgonians to verify that no significant changes occurred due to their presence in the chamber (Table S6). Organisms were transferred into 3-L cylindrical incubation flow chambers (see de Goeij et al. 2013 for a description of the chamber design) at 1–2 m horizontal and vertical distance to the slope to avoid intrusion of sediment. Some incubations with gorgonians were performed in larger (6-L), but otherwise equal chambers. Chamber lids were equipped with a magnetic stirrer to ensure constant mixing, an optical oxygen probe (Onset HOB0 Pendant U-26, calibrated using a two-point calibration of 0 and 100 % O₂ seawater solutions) to continuously monitor oxygen evolution (one measurement per min to determine productivity and respiration), and two sampling ports consisting of flexible tubing, all of which was inserted through airtight ports in the chamber lid. Incubation chambers, glassware, sample syringes and tubes were submerged in 0.4 mol L⁻¹ HCl for 12 h and subsequently rinsed with ultrapure water (18.2 MΩ-cm type I, Elga Purelab Classic UV) and 0.7 μm GF/F (47 mm, Whatman) filtered seawater (note: oxygen probes and stirrers were only rinsed in filtered seawater). Light incubations were performed around midday (10:00–14:00 hours) and chambers were placed at an angle of 45° to a horizontal plane, which ensured that light levels inside the chamber equaled ambient levels. Photosynthetic active radiation was measured using Odyssey PAR loggers (Dataflow Systems Limited, New Zealand, spectral detection range: 400–700 nm). Light incubations of cryptic rock and coralline algae were performed in shaded chambers covered in three layers of black nylon pantyhose to mimic ambient light on cryptic surfaces during the day. Dark incubations were performed in the early mornings (06:00 – 10:00 hours), with chambers darkened using black trash bags and duct tape.

A sample of ambient reef water (4 L) was taken at the beginning of each incubation to measure concentrations of suspended particulate C. Seawater samples from inside the chambers were sucked through the tubing into 100 mL syringes at the beginning, after 45–60 min, and at the end of incubations (after 4–5 h) to determine concentrations of dissolved C, pelagic bacteria, and phytoplankton communities. Incubation chambers were brought to the laboratory within 15 min and the chamber water (~ 3 L) was sampled for analysis of suspended particulate C within 1 hour of collection. All incubated organisms except algae were promptly extracted from chambers upon breaching the water surface and placed back onto the reef. Algae were extracted from chambers on land, rinsed quickly in ultrapure water to remove excess salts, frozen for 4 h at -20 °C, and

freeze-dried for 24 h (Scanvac Coolsafe 55-4, Labogene). Dried specimens were weighed on a precision scale (± 0.01 mg) to determine dry weight (DW), then combusted at 550 °C for 5 h and weighed again to determine ash weight. Ash-free dry weight (AFDW) was calculated by subtracting ash weight from DW. The remaining incubated fauna was mounted back to the reef and AFDWs were estimated from surface areas and volumes using available conversion factors (Kornder et al. 2021).

Finally, metabolic rates and fluxes of organic C by sponges were largely obtained from the literature (Table S1), however, the data set was complimented with our own measurements of respiration of three common species of massive sponges ($n = 3-12$, Table S2). Measurements were conducted during the day in March and April 2019 using the InEx technique (Yahel et al. 2005) with the same oxygen loggers that were employed in our incubations.

Laboratory analyses

Samples for suspended particulate carbon were filtered onto GF/F filters (47 mm, Whatman), freeze-dried as described above, and stored in a desiccator for transportation to the University of Amsterdam. Here, filters were freeze-dried again and weighed on a precision scale (± 0.01 mg) to determine DW. To estimate the proportion of C (in $\text{mg C L}^{-1}\text{Seawater}$), filters were acidified with 4 mol L^{-1} HCl until effervescence ceased to remove inorganic carbon (Nieuwenhuize et al. 1994), before being analyzed on a carbon, hydrogen, nitrogen, and sulphur elemental analyzer (CHNS-EA; Elementar Vario El Cube). H, N, and S contents were not further analyzed for this study.

Duplicate samples of dissolved organic C (20 mL) were filtered on-site through in-line filter holders loaded with pre-combusted (550 °C, 5 h) GF/F filters (0.7 μm pore size, 25 mm, Whatman). Filter holders containing clean filters were flushed with 20 mL of each 0.4 mol L^{-1} HCl, milli-Q water, and sample water before filling pre-combusted 22 mL EPA vials with 20 mL of fresh sample filtrate. Vials were acidified with 4–5 drops of fuming HCl (37%) and stored in the dark at 4 °C. In Amsterdam, dissolved organic C concentration was measured by high-temperature combustion of the acidified filtrate in a total organic carbon analyzer (Shimadzu) as described by Campana et al. (2021). Samples of pelagic bacteria (1 mL) and phytoplankton (3.5 mL) were transferred to cryovials containing glutaraldehyde (2 % (v/v) final concentration) and a formaldehyde + hexamine solution (0.5 % (v/v) formaldehyde and 0.3 % (w/v) hexamine, final concentration), respectively. Vials were left in the dark for 1 h, flash-frozen in liquid nitrogen, and stored at -80 °C until being analyzed on a CytoFLEX flow cytometer (Beckman Coulter, USA). At medium flow rate (30 $\mu\text{L min}^{-1}$), 50 μL of diluted sample water (PBS buffer, bacteria: 1:4, phytoplankton: 1:3) were excited with a blue (488 nm) laser to count the abundances of bacteria (high- and low-nucleic acid bacteria), *Synechococcus*

spp. (*Syn*) and *Prochlorococcus* spp. (*Pro*). Counts were based on forward scatter, side scatter, and the following types of fluorescence: Bacteria were stained using SYBR Green I nucleic acid gel stain (Molecular Probes, Inc) as described earlier in Marie et al. (1997), and quantified based on green fluorescence. *Syn* were quantified by their phycoerythrin pigments (orange fluorescence), and *Pro* based on the red to low red fluorescence of their divinyl chlorophyll a. For each sample, planktonic C (in mg L^{-1}) was estimated as the sum of bacterial and phytoplankton C. Detrital C was estimated by subtracting planktonic C from particulate C.

Supplementary figures

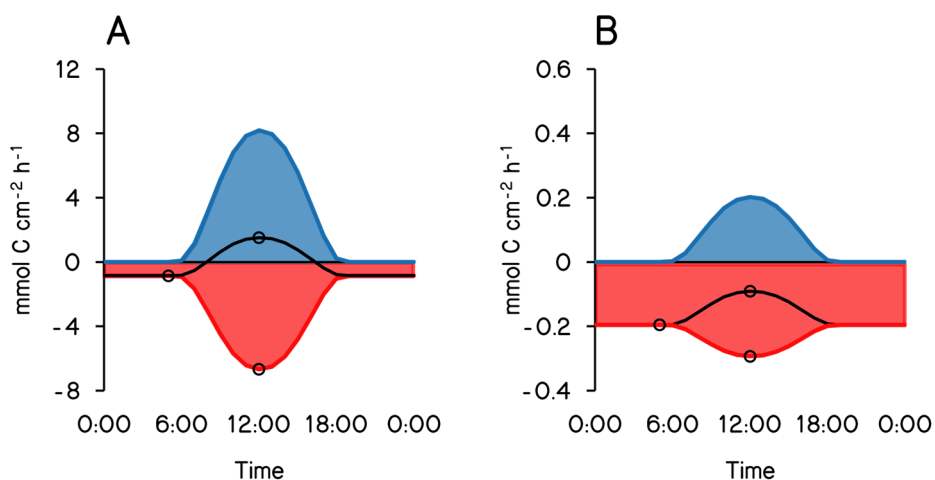


Figure S1. Assumed trajectory of hourly metabolic fluxes. Examples illustrate average rates of net phototrophic scleractinian corals (A) and net heterotrophic cryptic substrate (B) over the course of one day. Shown are hourly gross productivity (blue line), hourly net productivity (dashed line), hourly respiration (red line), and discrete sampling points (circles). The shape of the curve was obtained by averaging published estimates of hourly photosynthetically active radiation in the studied region (Curaçao) over the study period (April 2019 – December 2020) for each hour of the day (data available at power.larc.nasa.gov/data-access-viewer). Daily gross primary productivity (blue area) and daily respiration (red area) were estimated as definite integrals of the hourly rate functions.

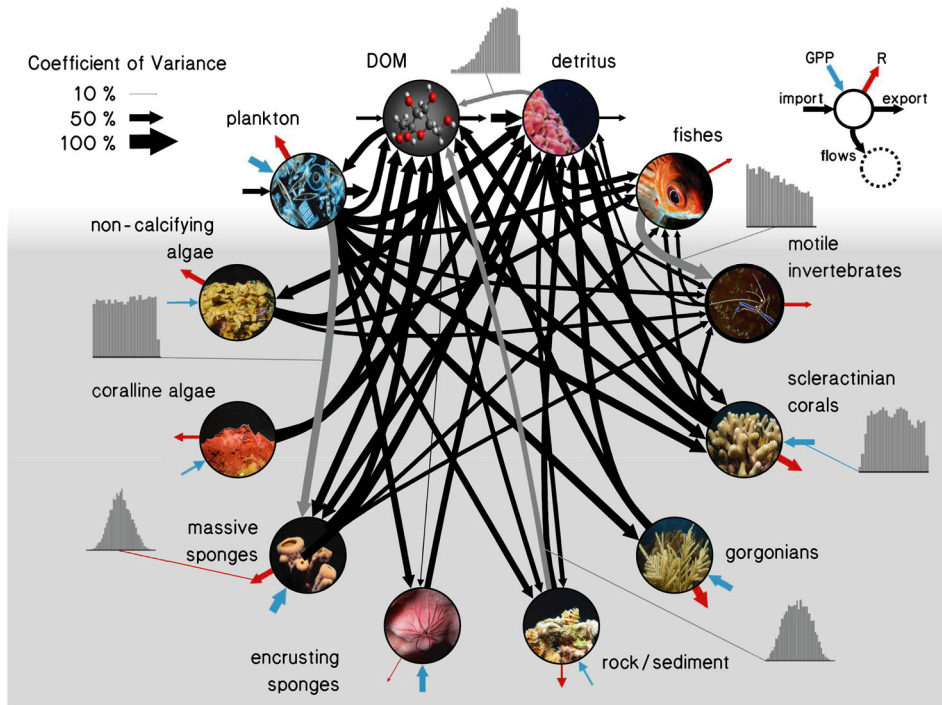


Figure S2. Sensitivities of carbon flows in a Caribbean coral reef. Background illustrates benthic (grey) and pelagic (white) compartments. Arrow widths correspond to coefficients of variance (see legend). Blue arrows are gross primary productivity, red arrows are respiration, horizontal arrows are import and export, and other arrows are C flows between (groups of) taxa (see Figure 4 for mean flow sizes). Histograms of model solutions for some selected flows are also shown (gray internal arrows). A summary of all flows and associated data sources is given in Table S5.

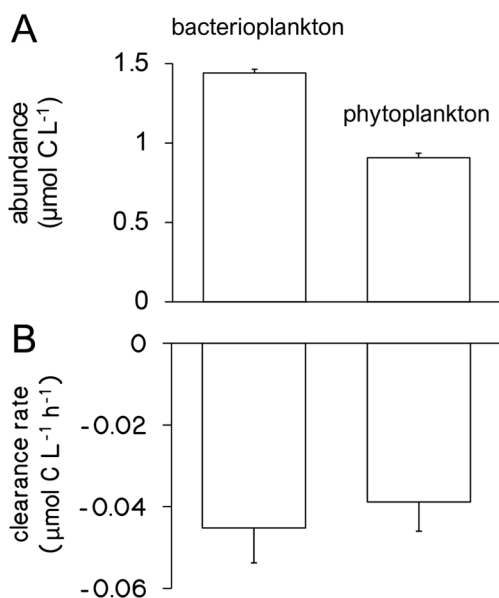


Figure S3. Average plankton abundances in *in-situ* incubations at $t = 0$ (**A**) and clearance rates of plankton by benthic organisms during incubations (**B**) on the leeward reef slope of Curaçao (mean \pm SE, $n = 130$). Carbon transfer to the benthos via consumption of heterotrophic bacterioplankton (i.e., the pelagic part of the microbial loop) was estimated as 60 % of the total consumption of plankton by benthic organisms.

Supplementary tables

Table S1. Meta-data set to supplement measurements of organic carbon (C) flows for model calibration. Sample size is given instead of the value when several observations were extracted. Number of studied species is given if multiple species were studied. Fluxes are uptake (negative) or release rates (positive). Elevated respiration ratios are given in daytime respiration/nighttime respiration. Photosynthetic quotients are mol O_2 produced/mol C assimilated. Respiratory quotients are mol CO_2 produced/mol O_2 consumed. PR, productivity to respiration ratio; min, minimum; max, maximum; photosyn., photosynthetic; respir., respiratory; WC, water column; DBL, diffusive boundary layer.

group/species	measure	value	unit	source
encrusting sponges				
<i>Xestospongia bocatorensis</i>	hourly P:R	1.14	ratio	(Freeman et al. 2013)
<i>Chondrilla caribensis</i>	hourly P:R	0.75	ratio	(Freeman et al. 2013)
<i>Chondrilla caribensis</i>	daily P:R	0.24	ratio	(Hudspith et al. 2022)
<i>Chondrilla caribensis</i>	respiration	$n = 6$	$\mu\text{mol O}_2 \text{ cm}^{-2} \text{ h}^{-1}$	(Hudspith et al. 2022)
3 species	respiration	$n = 9$	$\mu\text{mol O}_2 \text{ cm}^{-3} \text{ h}^{-1}$	(de Goeij et al. 2008b)
<i>Halichondria panicea</i>	respiration	0.52	$\mu\text{mol O}_2 \text{ cm}^{-3} \text{ h}^{-1}$	(Kumala and Canfield 2018)
<i>Neopretosia problematica</i>	respiration	0.83	$\mu\text{mol O}_2 \text{ cm}^{-3} \text{ h}^{-1}$	(Ludeman et al. 2017)
<i>Cliona delitrix</i>	respiration	0.31	$\mu\text{mol O}_2 \text{ cm}^{-3} \text{ h}^{-1}$	(Ludeman et al. 2017)
<i>Chondrilla caribensis</i>	plankton uptake	$n = 12$	$\mu\text{mol C cm}^{-2} \text{ h}^{-1}$	(Hudspith et al. 2022)
3 species	plankton uptake	$n = 33$	$\mu\text{mol C cm}^{-3} \text{ h}^{-1}$	(de Goeij et al. 2008b)
<i>Chondrilla caribensis</i>	dissolved C flux	$n = 6$	$\mu\text{mol C cm}^{-2} \text{ h}^{-1}$	(Hudspith et al. 2022)
3 species	dissolved C flux	$n = 32$	$\mu\text{mol C cm}^{-3} \text{ h}^{-1}$	(de Goeij et al. 2008b)
<i>Mycale fistulifera</i>	detritus flux*	0.65	$\mu\text{mol C cm}^{-3} \text{ h}^{-1}$	(Rix et al. 2018)

Carbon cycling in coral reefs: I. Net heterotrophy

group/species	measure	value	unit	source
<i>Negombata magnifica</i>	detritus flux*	0.72	$\mu\text{mol C cm}^{-3} \text{ h}^{-1}$	(Rix et al. 2018)
8 species	detritus flux	n = 30	percent of DW d ⁻¹	(Alexander et al. 2014)
<i>Halisarca caerulea</i>	detritus flux*	n = 30	$\mu\text{mol C mmol}^{-1} \text{ h}^{-1}$	(de Goeij et al. 2013)
massive sponges				
<i>Negombata magnifica</i>	respiration	310	$\text{nmol O}_2 \text{ min}^{-1} \text{ g}_{\text{AFDW}}^{-1}$	(Hadas et al. 2008)
review	respiration min	0.21	$\mu\text{mol O}_2 \text{ cm}^{-3} \text{ h}^{-1}$	(Osinga et al. 1999)
review	respiration max	24.6	$\mu\text{mol O}_2 \text{ cm}^{-3} \text{ h}^{-1}$	(Osinga et al. 1999)
<i>Haliclona oculata</i>	respiration	95.54	$\mu\text{mol O}_2 \text{ g}_{\text{DW}}^{-1} \text{ h}^{-1}$	(Koopmans et al. 2010)
<i>Dysidea avara</i>	respiration	9.25	$\mu\text{mol O}_2 \text{ g}_{\text{DW}}^{-1} \text{ h}^{-1}$	(Ribes et al. 1999)
<i>Mycale laxissima</i>	respiration	25.26	$\mu\text{mol O}_2 \text{ g}_{\text{DW}}^{-1} \text{ h}^{-1}$	(Reiswig 1973)
<i>Tectitethya crypta</i>	respiration	6.64	$\mu\text{mol O}_2 \text{ g}_{\text{DW}}^{-1} \text{ h}^{-1}$	(Reiswig 1973)
<i>Verongula reiswigi</i>	respiration	27.39	$\mu\text{mol O}_2 \text{ g}_{\text{DW}}^{-1} \text{ h}^{-1}$	(Reiswig 1973)
<i>Aplysina fistularis</i>	respiration	33.64	$\mu\text{mol O}_2 \text{ g}_{\text{DW}}^{-1} \text{ h}^{-1}$	(Reiswig 1981)
<i>Theonella swinhoei</i>	respiration	1.404	$\mu\text{mol O}_2 \text{ cm}^{-3} \text{ h}^{-1}$	(Yahel et al. 2003)
<i>Aplysina fistularis</i>	respiration	4.74	$\mu\text{mol O}_2 \text{ cm}^{-3} \text{ h}^{-1}$	(Reiswig 1981)
<i>Aplysina aerophoba</i>	respiration	1.25	$\mu\text{mol O}_2 \text{ cm}^{-3} \text{ h}^{-1}$	(Wehrli et al. 2007)
<i>Callyspongia vaginalis</i>	respiration	3.12	$\mu\text{mol O}_2 \text{ cm}^{-3} \text{ h}^{-1}$	(Ludeman et al. 2017)
<i>Tethya californiana</i>	respiration	0.23	$\mu\text{mol O}_2 \text{ cm}^{-3} \text{ h}^{-1}$	(Ludeman et al. 2017)
<i>Neopetrosia problematica</i>	respiration	0.38	$\mu\text{mol O}_2 \text{ cm}^{-3} \text{ h}^{-1}$	(Ludeman et al. 2017)
<i>Xestospongia muta</i>	respiration	1.4	$\text{mmol O}_2 \text{ dm}^{-3} \text{ h}^{-1}$	(Hoer et al. 2018)
<i>Xestospongia muta</i>	respiration	1.7	$\text{mmol O}_2 \text{ dm}^{-3} \text{ h}^{-1}$	(Hoer et al. 2018)
9 species	dissolved C flux	n = 17	$\text{nmol C s}^{-1} \text{ dm}^{-3}$	(McMurray et al. 2018)
<i>Xestospongia muta</i>	dissolved C flux	-2.10	$\text{mmol C dm}^{-3} \text{ h}^{-1}$	(Hoer et al. 2018)
<i>Xestospongia muta</i>	dissolved C flux	-1.70	$\text{mmol C dm}^{-3} \text{ h}^{-1}$	(Hoer et al. 2018)
<i>Theonella swinhoei</i>	dissolved C flux	-26	$\text{nmol C min}^{-1} \text{ cm}^{-3}$	(Yahel et al. 2003)
9 species	detritus flux	n = 17	$\text{nmol C s}^{-1} \text{ dm}^{-3}$	(McMurray et al. 2018)
9 species	plankton uptake	n = 17	$\text{nmol C s}^{-1} \text{ dm}^{-3}$	(McMurray et al. 2018)
<i>Theonella swinhoei</i>	plankton uptake	4.20	$\text{nmol C min}^{-1} \text{ dm}^{-3}$	(Yahel et al. 2003)
6 species	hourly P:R	n = 6	ratio	(Thacker et al. 2007)
<i>Neopetrosia subtriangularis</i>	hourly P:R	2.5	ratio	(Erwin and Thacker 2008b)
<i>Aplysina fulva</i>	hourly P:R	0.53	ratio	(Erwin and Thacker 2008b)
<i>Aplysina fulva</i>	hourly P:R	0.43	ratio	(Freeman et al. 2013)
<i>Neopetrosia subtriangularis</i>	hourly P:R	1.81	ratio	(Freeman et al. 2013)
fishes				
classified by food source	biomass Curacao	128	gww m^{-2}	(WAITT-Institute 2017)
food web	biomass Honduras	191.85	gww m^{-2}	(Cáceres et al. 2016)
food web	biomass Caribbean	330.22	gww m^{-2}	(Opitz 1993)
food web	detritus flux	1.05	$\text{gww m}^{-2} \text{ d}^{-1}$	(Cáceres et al. 2016)
food web	detritus flux	0.77	$\text{gww m}^{-2} \text{ d}^{-1}$	(Opitz 1993)
large collection	detritus flux	1.56	mg C gww d^{-1}	(Bray et al. 1981)
Haemulidae	detritus flux	17.28	$\text{mmol C m}^{-2} \text{ d}^{-1}$	(Meyer and Schultz 1985)
Pomacanthidae	detritus flux	1.06	$\text{mmol C gww}^{-1} \text{ d}^{-1}$	(Klumpp and Polunin 1989)

group/species	measure	value	unit	source
food web	total consumption	7.32	gww m ⁻² d ⁻¹	(Cáceres et al. 2016)
food web	total consumption	12.52	gww m ⁻² d ⁻¹	(Opitz 1993)
Pomacanthidae	total consumption	1.90	mmol C gww ⁻¹ d ⁻¹	(Klumpp and Polunin 1989)
Pomacanthidae	total consumption	0.67	mmol C gww ⁻¹ d ⁻¹	(Klumpp and Polunin 1989)
<i>Sparisoma viride</i>	respiration	215.90	mg O ₂ kgww ⁻¹ h ⁻¹	(van Rooij and Videler 1996)
Teleostei	respiration min	157.88	mg O ₂ kgww ⁻¹ h ⁻¹	(Nilsson et al. 2007)
Teleostei	respiration max	849.85	mg O ₂ kgww ⁻¹ h ⁻¹	(Nilsson et al. 2007)
Teleostei	respiration max	367.97	mg O ₂ kgww ⁻¹ h ⁻¹	(Roche et al. 2013)
Teleostei	tissue DW/WW	0.22	ratio	(Stickney and Torres 1989)
Teleostei	tissue AFDW/WW	0.17	ratio	(Stickney and Torres 1989)
Teleostei	feces DW/WW	0.36	ratio	(Brett 1979)
Teleostei	feces C/WW	0.20	ratio	(Childress et al. 1990)
Teleostei	feces C/DW	0.40	ratio	(McGhie et al. 2000)
Teleostei	feces C/DW	0.32	ratio	(McGhie et al. 2000)
Teleostei	feces C/DW	0.07	ratio	(Saba and Steinberg 2012)
Teleostei	feces C/DW	0.06	ratio	(Staresinic et al. 1983)
motile invertebrates				
food web	biomass Honduras	404.24	gww m ⁻²	(Cáceres et al. 2016)
food web	biomass Caribbean	1480	gww m ⁻²	(Opitz 1993)
food web	detritus flux	3.63	gww m ⁻² d ⁻¹	(Cáceres et al. 2016)
food web	detritus flux	7.60	gww m ⁻² d ⁻¹	(Opitz 1993)
food web	total consumption	15.52	gww m ⁻² d ⁻¹	(Cáceres et al. 2016)
food web	total consumption	23.63	gww m ⁻² d ⁻¹	(Opitz 1993)
<i>Coralliophila abbreviata</i>	respiration	1.05	mg O ₂ gAFDW ⁻¹ h ⁻¹	(Baums et al. 2003)
Polychaeta	respiration	96	mg O ₂ kgww ⁻¹ h ⁻¹	(Sander 1967)
<i>Tripteneustes gratilla</i>	respiration min	4.50	μmol C gDW ⁻¹ h ⁻¹	(Dy et al. 2002)
<i>Tectus niloticus</i>	respiration min	8.30	μmol C gAFDW ⁻¹ h ⁻¹	(Lorrain et al. 2015)
Crustacea, Echinodermata	respiration min	0.04	μmol O ₂ gww ⁻¹ h ⁻¹	(Wilson et al. 2013)
<i>Tripteneustes gratilla</i>	respiration max	27.2	μmol C gDW ⁻¹ h ⁻¹	(Dy et al. 2002)
<i>Tectus niloticus</i>	respiration max	14.8	μmol C gAFDW ⁻¹ h ⁻¹	(Lorrain et al. 2015)
<i>Musculista senhousia</i>	respiration max	200	mg O ₂ gDW ⁻¹ d ⁻¹	(Inoue and Yamamuro 2000)
Crustacea, Echinodermata	respiration max	2.70	μmol O ₂ gww ⁻¹ h ⁻¹	(Wilson et al. 2013)
motile invertebrates	feces AFDW/DW	0.24	ratio	(Graf and Rosenberg 1997)
motile invertebrates	feces AFDW/DW	0.09	ratio	(Klumpp and Pulfrich 1989)
motile invertebrates	feces C/DW	0.10	ratio	(Kraeuter 1976)
<i>Calianassa sp.</i>	feces C/DW	0.07	ratio	(Frankenberg et al. 1967)
metabolic scaling				
<i>Stylophora pistillata</i>	elevated R	1.8	ratio	(Porter et al. 1984)
<i>Porites porites</i>	elevated R	1.39	ratio	(Edmunds and Davies 1988)
<i>Favia sp., Acropora sp.</i>	elevated R	6.7	ratio	(Kühl et al. 1995)
<i>Pavona decussata</i>	elevated R	11	ratio	(Schrammeyer et al. 2014)
<i>Pocillopora damicornis</i>	elevated R	25	ratio	(Schrammeyer et al. 2014)
8 coral species	elevated R	1	ratio	(Comeau et al. 2017)
<i>Chondrus crispus</i>	elevated R	2	ratio	(Furbank and Rebeille 1986)
<i>Lithophyllum cabiochae</i>	elevated R	1.5	ratio	(Martin et al. 2013)
reef community	elevated R	2.2	ratio	(Langdon and Atkinson 2005)
sediment communities	elevated R	1.6	ratio	(Boucher et al. 1998)
plankton	elevated R	3.5	ratio	(Pringault et al. 2007)

Carbon cycling in coral reefs: I. Net heterotrophy

group/species	measure	value	unit	source
<i>Stylophora sp.</i>	photosyn. quotient	1.45	ratio	(Gattuso and Jaubert 1990)
<i>Eunicella singularis</i>	photosyn. quotient	1.10	ratio	(Ferrier-Pagès et al. 2015)
<i>Ellisolandia elongata</i>	photosyn. quotient	1.22	ratio	(Guy-Haim et al. 2016)
<i>Porolithon onkodes</i>	photosyn. quotient	1.21	ratio	(Chisholm et al. 1990)
macroalgal reef	photosyn. quotient	1.10	ratio	(Gattuso et al. 1996)
<i>Laminaria longicruris</i>	photosyn. quotient	1.19	ratio	(Hatcher et al. 1977)
5 macroalgae species	photosyn. quotient	0.75	ratio	(Rosenberg et al. 1995)
turf algae	photosyn. quotient	1.04	ratio	(Carpenter and Williams 2007)
sediment communities	photosyn. quotient	0.90	ratio	(Taddei et al. 2008)
plankton	photosyn. quotient	1.20	ratio	(Strickland 1960)
plankton	photosyn. quotient	1.95	ratio	(Williams and Raine 1979)
<i>Pocillopora sp., Fungia sp.</i>	respir. quotient	0.80	ratio	(Muscatine et al. 1981)
<i>Stylophora sp.</i>	respir. quotient	0.84	ratio	(Gattuso and Jaubert 1990)
<i>Eunicella singularis</i>	respir. quotient	0.80	ratio	(Ferrier-Pagès et al. 2015)
<i>Ellisolandia elongata</i>	respir. quotient	1.10	ratio	(Guy-Haim et al. 2016)
macroalgal reef	respir. quotient	0.76	ratio	(Gattuso et al. 1996)
sediment communities	respir. quotient	1.00	ratio	(Taddei et al. 2008)
sediment communities	respir. quotient	1.35	ratio	(Boucher et al. 1998)
plankton	respir. quotient	0.80	ratio	(Robinson et al. 2002)
Teleosteidae	respir. quotient	0.73	ratio	(Price and Mager 2020)
motile invertebrates	respir. quotient	0.75	ratio	(Hatcher 1989)
hydrodynamics				
hydrodynamics	current speed WC	11.5	cm s ⁻¹	(van Duyl et al. 2006)
hydrodynamics	current speed DBL n = 12		cm s ⁻¹	(Stocking et al. 2016)
hydrodynamics	current speed DBL > 1		cm s ⁻¹	(Larkum et al. 2003)
hydrodynamics	DBL thickness	1.20	cm	(Brown and Carpenter 2013)
hydrodynamics	3D reef rugosity	2.71	m ² mreef ⁻²	(Kornder et al. 2021)

Table S2. Respiration rates and associated measurements of three massive sponges using the InEx technique. rp, replicate; d, depth; Sv, sponge volume; Oa, osculum area; Pv, pumping velocity; O₂ ex, dissolved oxygen concentration of exhaled seawater; O₂ in, dissolved oxygen concentration of inhaled seawater; C, organic carbon. Asterisks denote outliers.

species	rp	d [m]	Sv [L]	Oa [cm ²]	Pv [cm s ⁻¹]	O₂ ex [μmol O ₂ L ⁻¹]	O₂ in [μmol O ₂ L ⁻¹]	respiration [mmol C L _{sponge} ⁻¹ h ⁻¹]
<i>Aplysina archeri</i>	1	5.7	0.31	5.74	7.20	247.81	262.78	6.64
	2	5.7	0.31	5.74	3.60	232.78	261.15	6.29
	3	8.0	0.81	30.45	3.09	147.74	267.64	46.42*
	4	8.0	0.51	2.70	5.84	247.94	255.81	0.82
	5	9.2	0.76	13.99	3.13	244.38	262.71	3.52
	6	19.1	1.26	10.40	8.31	196.60	252.92	12.91
	7	8.3	0.76	8.06	8.00	153.91	260.55	30.47*
	8	7.5	1.20	16.36	9.00	230.31	259.06	11.83
	9	19.9	2.13	17.98	7.20	239.34	256.70	3.53
	10	11.9	1.06	14.51	10.29	242.16	259.22	8.05
	11	6.5	0.30	9.87	12.00	243.91	266.72	29.93*
	12	18.7	1.15	15.83	6.75	237.36	258.96	6.73
<i>Callyspongia vaginalis</i>	1	16.8	0.07	5.25	8.31	259.09	261.28	4.71
	2	13.7	0.08	12.30	1.70	260.91	262.56	1.44
	3	11.9	0.14	28.62	2.16	260.91	262.56	2.53
<i>Callyspongia plicifera</i>	1	22.0	0.95	38.39	6.17	257.41	263.15	4.79
	2	17.8	0.20	47.89	6.97	260.76	265.00	23.34*
	3	13.2	0.84	20.07	4.08	260.23	271.91	3.79
	4	11.2	0.51	23.61	4.50	261.67	262.95	0.90
	5	12.2	0.48	17.69	3.93	257.62	263.71	2.98

Table S3. Overview of incubated species and benthic groups. Biomass conversions are given in $\text{g}_{\text{AFDW}} \text{cm}^{-2}$ (scleractinian corals and coralline algae) or $\text{g}_{\text{AFDW}} \text{cm}^{-3}$ (gorgonians). “coral rock” contained mainly endolithic algae, excavating sponges, and polychaetes. “cryptic rock” contained cryptic taxa other than coralline algae and sponges (predominantly tunicates, bivalves, bryozoans, and hydrozoans). Reef water samples were taken between 0.1 and 5 m above the benthos. Seawater samples were taken 1 km offshore at 1.5 m depth. Sponges were not incubated because their C fluxes were available from recent measurements using the same methodology as this study (Table S1).

group	species	biomass conversion	n	
			light	dark
scleractinian corals	<i>Colpophyllia natans</i>	0.086719	9	6
	<i>Madracis mirabilis</i>	0.099467	7	6
	<i>Orbicella faveolata</i>	0.137871	6	6
	<i>Agaricia lamarckii</i>	0.137871	6	6
gorgonians	<i>Eunicea sp.</i>	0.089964	6	6
	<i>Plexaura sp.</i>	0.089964	5	6
coralline algae	crustose coralline algae	0.01525 ± 0.00279	10	7
non-calcifying phototrophs	<i>Dictyota spp.</i>		8	8
	<i>Lobophora spp.</i>		9	7
rock / sediment communities	coral rock		6	6
	cryptic rock		6	6
	sediment		6	6
plankton	unfiltered seawater		12	8
	dolerite controls		6	6
externals	reef water		21	
	off-shore ocean water		15	

Table S4. Summary of linear regression models testing for significant trends (p-value < 0.05, bolded) of different C sources over time in light and dark incubations containing only seawater. O₂ measurements were converted to C using a photosynthetic quotient of 1.19 for light incubations and a respiratory quotient of 0.93 for dark incubations (see Table S1 for relevant literature). df, degrees of freedom; resSE, residual standard error; R²adj, adjusted R²; n, sample size.

source	type	flux	df	F	t	p-value	R ² adj	n
		[$\mu\text{mol C L}^{-1} \text{ h}^{-1}$]						
dissolved	light	4.80	21	1.78	1.34	0.20	0.08	15
organic C	dark	5.02	22	1.89	1.37	0.18	0.04	13
planktonic C	light	-0.32	19	13.26	-3.64	<0.01	0.38	14
	dark	-0.11	14	0.63	-0.79	0.44	-0.03	9
detrital C	light	0.65	8	0.27	0.52	0.62	-0.09	9
	dark	0.65	6	0.51	0.71	0.50	-0.08	7
O ₂	light	-0.19	3221	80.88	-8.99	<<0.01	0.02	12
	dark	-0.44	2532	119.90	-10.95	<<0.01	0.05	10

Table S5. Predicted organic carbon (C) flows (in $\text{mmol C m}^{-2} \text{ d}^{-1}$) of the individual functional groups and whole community on the reef slope (9–14 m depth) of Curaçao (leeward shore) using linear inverse modeling. DOM, dissolved organic matter. “source” depicts main source of data for each flow, i.e., our own *in-situ* measurements (source in Table 1) or literature data (source in Table S1). “ID” corresponds to the C flow abbreviations in Box 1. Note that 95-percentile ranges of whole-community fluxes are derived from their own sets of model solutions and are therefore narrower than the ranges obtained by adding the flux limits of individual functional groups.

group	mean	SD	95-percentile range		source	ID
	[$\text{mmol C m}^{-2} \text{ d}^{-1}$]		lower limit	upper limit		
gross primary productivity						
plankton	67.58	34.41	6.38	128.83	1	GPPpl
non-calcifying phototrophs	343.77	44.82	253.92	414.64	1	GPPma
coralline algae	32.36	5.30	21.17	40.31	1	GPPca
rock / sediment	60.50	8.57	45.25	75.97	1	GPPrsc
gorgonians	716.11	329.08	178.19	1208.26	1	GPPgc
scleractinian corals	572.29	231.14	190.41	971.60	1	GPPsc
massive sponges	74.58	42.91	5.89	144.11	S1	GPPms
encrusting sponges	22.49	9.66	5.59	39.95	S1	GPPes
total community	1889.6	407.71	1120.53	2655.80		
net primary productivity						
plankton	-29.53	55.88	-136.05	77.61	1	
non-calcifying phototrophs	160.46	43.19	84.61	244.96	1	
coralline algae	9.76	4.18	2.11	18.16	1	
rock / sediment	1.66	3.46	-4.86	8.25	1	
gorgonians	123.46	54.39	32.13	220.85	1	
scleractinian corals	91.14	39.70	20.76	172.93	1	
massive sponges	-127.78	63.20	-245.45	-12.20	S1	
encrusting sponges	-470.87	28.90	-523.097	-411.702	S1	
total community	-336.48	86.20	-506.91	-166.38		

Carbon cycling in coral reefs: I. Net heterotrophy

group	mean [mmol C m ⁻² d ⁻¹]	SD	95-percentile range		source	ID
			lower limit	upper limit		
P:R ratio						
plankton	1.00	1.28	0.06	4.20	1	
non-calcifying phototrophs	2.15	0.80	1.31	4.20	1	
coralline algae	1.47	0.25	1.08	2.04	1	
rock / sediment	1.03	0.06	0.92	1.15	1	
gorgonians	1.37	0.43	1.04	2.67	1	
scleractinian corals	1.27	0.23	1.04	1.91	1	
massive sponges	0.38	0.22	0.05	0.85	S1	
encrusting sponges	0.05	0.02	0.01	0.08	S1	
total community	0.84	0.05	0.74	0.93		
respiration						
plankton	97.11	41.55	20.45	177.81	1	Rpl
non-calcifying phototrophs	183.31	69.50	69.52	294.58	1	Rma
coralline algae	22.59	5.00	15.06	40.31	1	Rca
rock / sediment	58.84	8.24	44.89	73.06	1	Rrsc
gorgonians	592.65	329.33	81.34	1121.93	1	Rgc
scleractinian corals	481.15	230.80	115.68	888.46	1	Rsc
massive sponges	202.36	80.94	48.90	358.21	1, S1	Rms
encrusting sponges	493.36	26.45	438.32	539.05	S1	Res
motile invertebrates	56.90	11.45	29.72	58.58	S1	Rmi
fishes	37.88	13.72	12.61	71.40	S1	Rf
total community	2226.1	413.98	1440.36	3000.15		
DOM production						
plankton	132.94	63.89	21.89	263.36	1	DOMPpl
non-calcifying phototrophs	67.71	38.60	5.09	147.00	1	DOMPma
coralline algae	4.43	2.78	0.21	9.47	1	DOMPca
rock / sediment	8.12	3.09	2.44	13.92	1	DOMPrsc
gorgonians	96.35	50.98	18.11	182.61	1	DOMPgc
scleractinian corals	53.12	29.40	3.57	104.91	1	DOMPsc
massive sponges	17.87	10.30	0.86	34.79	S1	DOMPms
total community	380.53	83.06	224.77	547.08		
DOM consumption						
plankton	155.64	76.57	16.54	289.37	1	DOMCpl
non-calcifying phototrophs	0.44	0.26	0.02	0.87	1	DOMCma
coralline algae	0.60	0.35	0.03	1.17	1	DOMCca
rock / sediment	1.33	0.46	0.42	2.13	1	DOMCrsc
scleractinian corals	5.56	3.16	0.29	10.79	1	DOMCsc
massive sponges	86.32	50.31	4.25	167.50	S1	DOMCms
encrusting sponges	463.03	26.69	414.09	518.28	S1	DOMCes
total community	712.93	83.42	554.09	872.60		
detritus production						
plankton	99.72	59.61	4.82	202.73	1	DPpl
coralline algae	5.94	3.33	0.94	12.20	1	DPca
rock / sediment	2.80	1.18	0.77	5.28	1	DPsc
gorgonians	28.12	15.63	3.79	55.39	1	DPgc
scleractinian corals	35.81	25.63	1.55	97.06	1	DPsc
massive sponges	15.10	9.14	0.73	30.87	S1	DPms
encrusting sponges	59.26	25.86	25.17	118.69	S1	DPes
motile invertebrates	12.54	2.73	7.85	16.83	S1	DPmi
fishes	75.21	24.39	28.97	124.38	S1	DPf
total community	334.49	45.25	242.01	417.27		

Chapter 4

group	mean [mmol C m ⁻² d ⁻¹]	SD	95-percentile range		source	ID
			lower limit	upper limit		
detritus consumption						
rock / sediment	7.40	2.38	2.77	11.97	1	DCrsc
scleractinian corals	0.46	0.27	0.03	0.91	1	DCsc
massive sponges	33.54	17.99	1.97	61.42	S1	DCms
motile invertebrates	32.08	9.64	18.11	51.60	S1	DCmi
fishes	10.74	4.42	3.44	18.00	S1	DCf
total community	84.24	20.97	45.19	122.83		
grazing on plankton and macroalgae						
rock / sediment	0.53	0.23	0.10	0.90	1	PLGrsc
gorgonians	1.01	0.58	0.05	1.96	1	PLGgc
scleractinian corals	1.74	1.02	0.08	3.43	1	PLGsc
massive sponges	50.89	28.34	3.75	96.65	S1	PLGm
encrusting sponges	67.10	30.99	13.05	132.16	S1	PLGes
motile invertebrates	56.77	11.75	38.42	83.51	S1	PLGmi+AGmi
fishes	62.96	21.05	32.89	112.64	S1	PLGf + AGf
total community	240.99	46.66	154.37	335.26		
predation						
motile invertebrates	22.44	5.53	12.37	33.25	S1	PRx,mi
fishes	46.53	10.58	22.35	61.26	S1	PRx,f
total community	68.97	12.43	41.47	89.00		
import						
detritus	32.05	19.67	1.38	67.11	1	IMPdet
DOM	901.55	202.99	601.52	1233.16	1	IMPdom
plankton	262.83	92.97	71.73	425.19	1	IMPpl
total community	1196.4	202.04	865.52	1568.53		
export						
detritus	186.57	32.86	110.38	230.01	1	EXPdet
DOM	664.89	193.27	375.48	998.59	1	EXPdom
plankton	8.49	4.87	0.44	16.51	1	EXPpl
total community	859.95	196.62	560.20	1204.88		

Table S6. Summary of Mann-Whitney-U test results checking for significant differences (p -value < 0.05) in hourly C fluxes (medians given in $\mu\text{mol C L}^{-1} \text{ h}^{-1}$) measured in blank controls versus controls containing dolerite bases (3 L chamber volume). O_2 fluxes were converted to C using a photosynthetic quotient of 1.19 for light incubations and a respiratory quotient of 0.93 for dark incubations (Table S1). No significant difference was found. Data were merged to control for seawater in experimental incubations.

source	type	blank controls		dolerite controls		W	p-value
		median	n	median	n		
dissolved organic C	light	2.23	9	3.15	6	19	0.39
	dark	1.34	8	1.91	5	20	1.00
planktonic C	light	-0.09	8	-0.07	5	16	0.62
	dark	-0.01	4	-0.03	5	10	1.00
detrital C	light	0.14	4	0.17	5	10	1.00
	dark	0.38	3	0.10	4	7	0.86
O_2	light	-0.02	6	-0.36	4	19	0.17
	dark	0.06	9	-0.23	3	23	0.10

Supplementary data & code

This chapter contains supplementary data and code, available at figshare.com (DOI: 10.21942/uva.22592536). Additional requests regarding these resources should be directed to and will be fulfilled by the lead contact, Niklas A. Kornder (niklaskornder@googlemail.com).

Data S1. Raw measurements of the C concentrations during incubations and in reef water in $\mu\text{mol C L}^{-1}$. The initial “read me” tab provides descriptions of abbreviated terms and applicable conversion factors. The following tabs each list the raw measurements for a particular functional group. The last two tabs list the values measured during incubations containing only seawater (i.e., functional group plankton) and the C concentrations in seawater from the reef versus open ocean.

Data S2. Raw measurements of the dissolved O_2 concentrations during incubations of benthic reef organisms in mg L^{-1} . Individual tabs list all incubations for a particular functional group and incubation time (light = at midday, dark = at night). The first column denotes time (in minutes) followed by dissolved O_2 concentrations, temperatures (in $^{\circ}\text{C}$) and, where available, light irradiances (in par) for individual replicate incubations.

Data S3. Output of the linear-inverse model for the leeward reef slope of Curaçao (between 9–14 m water depth). Each column represents a single flow of C between

two compartments of the model and lists all 10000 model solutions for that flow. See Box 1 for a description of the abbreviations of the functional groups.

Code S1. This R script runs a linear-inverse model with 9999 iterations using the *LIM* package (Soetaert and van Oevelen 2009) and information stored in the script “file_name.input” (see Code S2). The model output is exported into R’s current directory as a csv file titled “model_output.csv”.

Code S2. This R script defines ranges and relationships for the carbon flows of the linear-inverse model presented in this chapter. The text can be saved in R’s current directory as “file_name.input” to rerun the model using Code S1. The text behind exclamation marks is purely descriptive. The structural elements of the script are explained in Soetaert & van Oevelen (2009).